

## Review Article

# Prostate-Specific Membrane Antigen as Target for Neuroimaging of Central Nervous System Tumors

**Brittany M. Stopa** <sup>1,2</sup> **James Crowley** <sup>3</sup> **Csaba Juhász** <sup>4,5</sup> **Cara M. Rogers** <sup>1,2,6</sup>  
**Mark R. Witcher** <sup>1,2,6</sup> and **Jackson W. Kiser** <sup>3</sup>

<sup>1</sup>Virginia Tech Carilion School of Medicine, Roanoke, VA, USA

<sup>2</sup>Fralin Biomedical Research Institute, Roanoke, VA, USA

<sup>3</sup>Carilion Clinic Radiology, Roanoke, VA, USA

<sup>4</sup>Departments of Pediatrics, Neurology, Neurosurgery, Wayne State University School of Medicine, Detroit, MI, USA

<sup>5</sup>PET Center and Translational Imaging Laboratory, Children's Hospital of Michigan, The Karmanos Cancer Institute, Detroit, MI, USA

<sup>6</sup>Carilion Clinic Neurosurgery, Roanoke, VA, USA

Correspondence should be addressed to Jackson W. Kiser; jwkiser@carilionclinic.org

Received 7 January 2022; Accepted 24 March 2022; Published 15 April 2022

Academic Editor: Henry VanBrocklin

Copyright © 2022 Brittany M. Stopa et al. This is an open access article distributed under the Creative Commons Attribution License, which permits unrestricted use, distribution, and reproduction in any medium, provided the original work is properly cited.

**Introduction.** Positron emission tomography (PET) imaging with prostate-specific membrane antigen- (PSMA-) binding tracers has been found incidentally to demonstrate uptake in CNS tumors. Following the encouraging findings of several such case reports, there is a growing interest in the potential application of PSMA-targeted PET imaging for diagnostics, theranostics, and monitoring of CNS tumors. This is a systematic literature review on PSMA-binding tracers in CNS tumors. **Methods.** A PubMed search was conducted, including preclinical and clinical reports. One hundred and twelve records were identified, and after screening, 56 were included in the final report. **Results.** Tissue studies demonstrated PSMA expression in tumor vascular endothelial cells, without expression in normal brain tissue, though the extent and intensity of staining varied by anti-PSMA antibody and methodology. Most included studies reported on gliomas, which showed strong PSMA ligand uptake and more favorable tumor to background ratios than other PET tracers. There are also case reports demonstrating PSMA ligand uptake in prostate cancer brain metastases, nonprostate cancer brain metastases, and meningiomas. We also review the properties of the various PSMA-binding radiotracers available. Therapeutic and theranostic applications of PSMA-binding tracers have been studied, including labeled alpha- and beta-ray emitting isotopes, as well as PSMA targeting in directing MRI-guided focused ultrasound. **Conclusions.** There is a potential application for PSMA-targeted PET in neuro-oncology as a combination of diagnostic and therapeutic use, as a theranostic modality for managing CNS tumors. Further research is needed regarding the mechanism(s) of PSMA expression in CNS tumors and its differential performance by tumor type.

## 1. Introduction

Standard imaging of central nervous system (CNS) tumors with magnetic resonance imaging (MRI) has demonstrated limitations [1], and positron emission tomography (PET) has emerged as an additional prominent noninvasive imaging modality for CNS tumors. Among the PET tracers under investigation for imaging of CNS tumors is prostate-specific membrane antigen (PSMA) binding tracer, whose utility in

the CNS was originally noted on PET scans of patients with prostate cancer [2–4]. PSMA is a type II transmembrane glycoprotein that was originally identified due to its high expression in malignant prostate vasculature. Subsequent research has revealed that it is also expressed in a variety of other tissue types in different organ systems [2, 4, 5]. PSMA is also known as glutamate carboxypeptidase II (GCPII) in the brain, as well as folate hydrolase I in the intestines [6], where its main enzymatic function is to cleave N-acetyl-L-aspartyl-L-glutamate

(NAAG) to N-acetylaspartate and glutamate [7]. In the normal rodent and human brain, astrocytes demonstrate some GCPII expression, which provides the majority of NAAG-hydrolyzing activity [6, 8], implicating this enzyme in some neuropsychiatric conditions in which glutamate is considered neurotoxic. As a result, inhibition of GCPII was thought to be neuroprotective, and GCPII inhibitor administration increased brain NAAG levels, improving cognitive performance in mice with experimental autoimmune encephalomyelitis [9]. Interestingly, efforts to develop small molecule inhibitors of GCPII to treat brain disorders of hyperglutamatergic pathogenesis led to the discovery of their application outside of the nervous system, most prominently as imaging and therapeutic agents in prostate cancers [10].

PET radioligands targeting PSMA are misleading in their nomenclature as “PSMA tracers,” because they are in reality inhibitors with high affinity for the PSMA-binding motif [11]. Such PSMA-targeting tracers have in recent years garnered greater interest because of their potentially widespread oncologic diagnostic applications, as well as therapeutic applications including those recently developed for prostate cancer. Importantly, PSMA is shown to have specific expression on tumor vasculature, which is unique from other vascular imaging tracers which nonspecifically bind to the vasculature in both normal tissue and tumor tissue, and this distinction may therefore facilitate direct targeting of tumor angiogenesis [12]. Case reports initially revealed the incidental finding of PSMA accumulation in CNS metastases, leading to subsequent exploration of PSMA expression and imaging in a variety of CNS malignancies. Here, we systematically review the literature investigating PSMA-targeted tracers for CNS lesions, including all identified *in vitro* and *in vivo* studies, in order to summarize current knowledge regarding the potential for PSMA-targeted PET in neuro-oncology imaging.

## 2. Methods

This review utilized a search strategy to identify previous preclinical and clinical research studies of PSMA-targeted PET in neuro-oncologic applications. The search was performed in the PubMed database (<https://pubmed.ncbi.nlm.nih.gov>) in May 2021 using the following search terms: ((brain tumor) OR (spine tumor) OR (CNS tumor) OR (neurooncology) OR (neuro-oncology) OR (glioblastoma) OR (glioma) OR (astrocytoma) OR (oligodendroglioma) OR (meningioma) OR (brain metastasis) OR (spine metastasis) OR (brain metastases) OR (spine metastases) OR (chordoma) OR (craniopharyngioma) OR (gangliocytoma) OR (glomus) OR (pineocytoma) OR (pituitary adenoma) OR (schwannoma) OR (acoustic neuroma) OR (ependymoma) OR (medulloblastoma) OR (hemangioblastoma) OR (rhabdoid)) AND ((positron emission tomography) OR (PET)) AND ((prostate specific membrane antigen) OR (PSMA)). All available years were included.

A total of 101 records were returned. The bibliographies of these papers were reviewed to elicit additional papers, yielding 11 additional articles. These 112 reports were then screened for original research publications related to PSMA

and neuro-oncology, including preclinical studies, retrospective and prospective clinical studies, and case reports, but excluding review papers, systematic reviews, and meta-analyses. This yielded 56 studies for inclusion in the final review. See the study selection flowchart in Figure 1.

Data collection and extraction were performed independently by one author (BS) with oversight by the other authors. Data variables collected included year, study design, study subjects, tumor type, tracer name, and main study results. Data were analyzed and summarized qualitatively.

## 3. Results

**3.1. Expression of PSMA in Tissue and Preclinical Models.** There are 13 published reports of PSMA expression in CNS tumor tissue and preclinical models, including a collective total of 331 patients and 38 animals (Table 1). The first such report was by Chang et al. (1999), in which the expression profile of several PSMA antibodies in a wide variety of tumor tissue types, among them a single glioblastoma (GBM), were examined [13]. They reported that GBM neovasculature cells stained PSMA-positive, while neither tumor cells nor normal brain demonstrated expression.

Wernicke et al. (2011) published an immunohistochemistry study of 32 GBMs, using an anti-SMA mAb 3E6 (Dako) stain, quantifying the extent and intensity of vascular endothelial staining [14]. They reported that all GBMs stained positive for PSMA, with variable extent and intensity. The extent of staining was mostly 51-100%, while the intensity of staining was mostly moderate or maximum. The PSMA staining colocalized within the areas of tumor with CD31, a known blood vessel marker, while, again, no staining was seen in any normal brain tissue.

The same group then published in 2014 a PSMA immunohistochemistry study of 14 breast cancer patients with brain metastases [15]. They used a mouse 3E6 anti-PSMA antibody (Dako) for immunohistochemistry staining and quantified the extent of staining in tumor-associated vessels. The tumor vasculature of all brain metastases stained PSMA-positive, and the extent of expression was greater than 50%. They also scored the primary tumor for 10 of these patients, and in all cases, the primary tumor had greater than 50% expression. That same year, Nomura et al. published a PSMA tissue study of 23 gliomas and breast cancer brain metastases [16]. They used a mouse PSMA antibody mAb 3E6 (Dako) for immunohistochemistry and quantified the intensity of PSMA staining in tissue relative to a staining calibration curve normalized to mean image background intensity, using the automated algorithms in the Scanscope® CM-1 scanner and ImageScope® software. They found that GBM blood vessels stained heavily, grade II/III gliomas showed some (<2%) tumor tissue staining but no vessel staining, and grade I gliomas showed moderate vessel staining and some tumor staining. They additionally found that normal tissue blood vessels did not stain for PSMA but fewer than 5% of normal neurons did. The quantified relative intensity of staining in all gliomas was statistically significantly higher than in normal brain. They also reported corresponding PSMA and von Willebrand factor

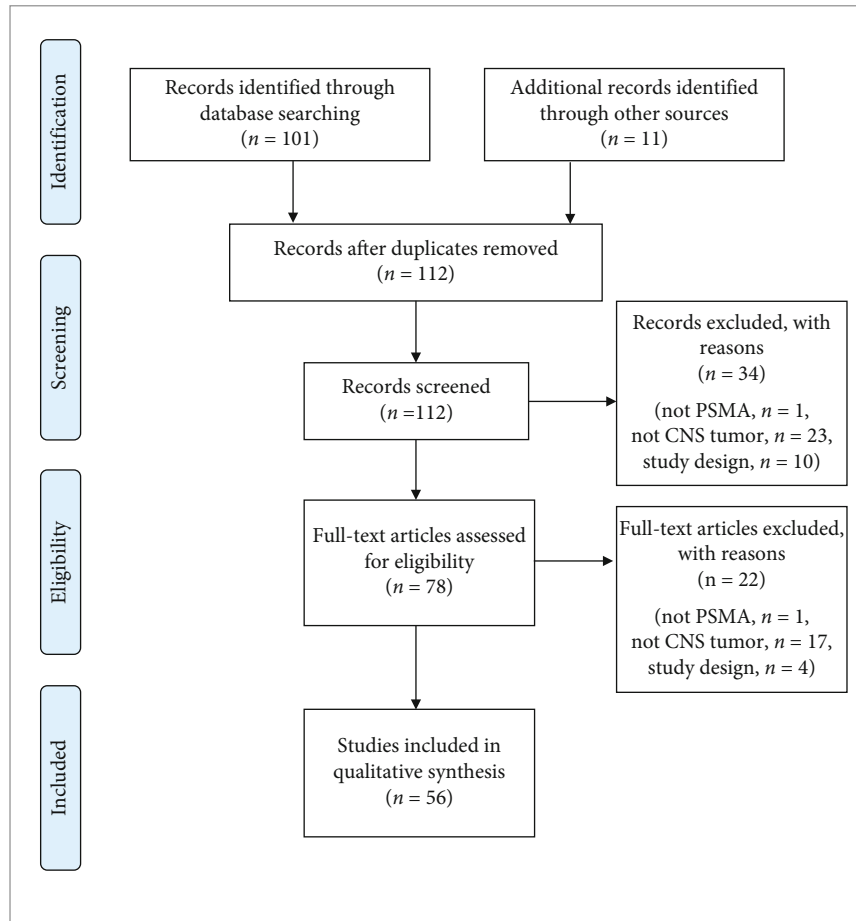


FIGURE 1: PRISMA study selection flowchart.

(VWF) staining on vascular endothelial cells. In brain metastases, they found variable staining within and between tumors, but on average the staining was significantly greater than normal brain.

The above data were complemented by several subsequent case reports. Schwenck et al. reported increased PSMA expression in the vascular endothelium of a GBM patient, though not in the normal brain and vasculature (Figure 2) [17]. Subsequently, Unterrainer et al. reported the first PSMA study in a gliosarcoma patient, which demonstrated strong PSMA expression in the neovascular endothelial cells and not in the tumor tissue cells [18]. Salas Fragomeni et al. reported in one anaplastic astrocytoma and 2 GBMs that PSMA staining was localized to the vascular cells in GBM and tumor cells in anaplastic astrocytoma, and no staining was found in normal brain or vessels [19].

The two largest of these studies, by Matsuda et al. [20] and Saffar et al. [21] were both published in 2018 and demonstrated divergent results regarding the expression of PSMA in high-grade gliomas. Matsuda et al. studied tissue samples from 78 glioma, brain metastasis, CNS lymphoma, and radiation necrosis patients [20]. They used a rabbit monoclonal anti-PSMA antibody (EPR6253, Abcam) for immunohistochemistry, and they quantified the strength of tissue PSMA expression in vascular endothelial cells. They

reported that PSMA was expressed in the vascular endothelial cells of almost all GBMs, most grade I and III gliomas, and all metastatic brain tumors. However, PSMA was expressed in few grade II gliomas and primary central nervous system lymphomas (PCNSL). They found no PSMA expression in radiation necrosis tissue. GBMs and brain metastases showed the highest expression levels, while few grade III gliomas and no grade II gliomas showed high expression. Saffar et al. reported on PSMA expression in 72 gliomas [21]. They used a monoclonal liquid Novocastra™ mouse monoclonal antibody (clone 1D6, Novocastra) for immunohistochemistry. They quantified the extent and intensity of PSMA staining in vascular endothelial cells. They found positive PSMA staining in a minority of gliomas, regardless of tumor grade. Among these, the GBMs and grade I gliomas had a lower extent of vascular staining, while the grade II and III gliomas had a higher extent of staining. The intensity of staining was weak for most of the GBMs and the grade III glioma, and it was moderate for the grade I and II gliomas.

The following year, Mahzouni et al. published a larger PSMA tissue study in GBMs ( $n = 60$ ) [22]. They used an anti-PSMA mAB clone SP29 (Biogenex) for immunohistochemistry and quantified the extent and intensity of PSMA staining in vascular endothelial cells. They found PSMA

TABLE 1: Summary of tissue expression of PSMA.

Authors	Year	<i>n</i>	Tumor type	Tissue stain	Main results
Chang et al.	1999	1	GBM	7E11 (Cytogen) J591 (homemade) J415 (homemade) PEQ226.5 (Hybritech) PM2J004.5 (Hybritech)	(i) All 5 anti-PSMA monoclonal antibodies react strongly with the neovasculature of GBM (ii) No expression in tumor cells or normal brain tissue
Wernicke et al.	2011	32	GBM	Mouse Ab 3E6 (Dako)	(i) 32/32 specimens stained for PSMA (ii) 7/32 had 75-100% vascular staining, 15/32 had 51-75% staining, 2/32 had 26-50% staining, and 8/32 had 1-25% staining (iii) 14/32 had 3+ staining intensity, 15/32 had 2+ intensity, and 3/32 had 1+ intensity (iv) No expression in the vessels of normal brain
Wernicke et al.	2014	14	Breast cancer brain metastases	Mouse Ab 3E6 (Dako)	(i) 14/14 had PSMA-positive expression in metastasis vasculature (ii) 14/14 had staining intensity of 2 (PSMA-positive in 50%+ tumor vessels)
Nomura et al.	2014	23	5 grade I gliomas 4 grade II gliomas 5 grade III gliomas 5 GBMs 4 breast cancer brain metastases	Mouse Ab 3E6 (Dako)	(i) Grade I gliomas: moderate tumor vascular staining, some tumor cell staining (ii) Grade II/III gliomas: light staining of some tumor cells (<2%), little/no vascular staining (iii) GBMs: heavy tumor vascular staining (iv) Breast cancer brain metastases: vascular staining, less than primary lesion, variable intensity within tumor (v) No expression in normal brain vasculature (vi) <5% expression in normal brain tissue
Schwenck et al.	2015	1	GBM	Unknown	(i) PSMA expression predominantly in tumor vascular endothelial cells (ii) No PSMA expression in normal brain tissue or vasculature
Unterrainer et al.	2017	1	Gliosarcoma	Unknown	(i) Strong PSMA expression in tumor vascular endothelial cells (ii) No expression in tumor tissue
Salas Fragomeni et al.	2017	3	1 anaplastic astrocytoma 2 GBMs	Unknown	(i) Anaplastic astrocytoma: PSMA expression localized to tumor cells (ii) GBMs: PSMA expression localized to tumor vasculature (iii) No expression in normal brain tissue or vasculature
Saffar et al.	2018	72	10 grade I gliomas 26 grade II gliomas 9 grade III gliomas 27 GBMs	Mouse Ab 1D6 (Novocastra)	(i) Grade I gliomas: 2/10 had PSMA expression, with staining intensity of 2; 8/10 had 0% extent of staining, 2 had 10-39% extent (ii) Grade II gliomas: 1/26 had PSMA expression, with staining intensity of 25/26 had 0% extent of staining, 1 had >70% extent (iii) Grade III gliomas: 1/9 had PSMA expression, with staining intensity of 1; 8/9 had 0% extent of staining, 1/9 had >70% extent (iv) GBMs: 11/27 had PSMA expression; 9/27 had staining intensity of 1, 1/27 had intensity of 2, 1/27 had intensity of 3; 16/27 had 0% extent of staining, 4/27 had 1-9% extent, 5/27 had 10-39% extent, 1/27 had 40-69% extent, 1/27 had >70% extent
Matsuda et al.	2018	78	4 grade I gliomas 7 grade II gliomas 15 grade III gliomas 41 GBMs 4 brain metastases 7 PCNSLs	Rabbit mAb EPR6253 (Abcam)	(i) Grade I gliomas: 3/4 had PSMA expression (ii) Grade II gliomas: 1/7 had PSMA expression; 0/7 with high expression (iii) Grade III gliomas: 10/15 had PSMA expression; 5/15 with high expression (iv) GBMs: 40/41 had PSMA expression; 32/41 with high expression (v) Brain metastases: 4/4 had PSMA expression; 3/4 with high expression

TABLE 1: Continued.

Authors	Year	<i>n</i>	Tumor type	Tissue stain	Main results
Mahzouni et al.	2019	60	GBM	Rabbit mAb SP29 (Biogenex)	(vi) PCNSLs: 2/7 had PSMA expression (vii) Radiation necrosis: 0/5 had PSMA expression (i) 40/60 with PSMA expression in tumor vasculature (ii) 3/60 with 76-100% extent of staining, 16/60 with 51-76% extent, 9/60 with 26-50% extent, 12/60 with 6-25% extent, 20/60 with <5% extent (iii) 15/60 with severe intensity of staining, 23/60 with moderate intensity, 7/60 with mild intensity, 15 with zero intensity (iv) No staining of normal brain vasculature
Oliveira et al.	2020	38*	Rat glioma (with F98, 9L, or U87 cells)	ab58779 (Abcam) NBP1-89822 (Novus) NBP1-45057 (Novus)	(i) Both <sup>68</sup> Ga-PSMA and <sup>18</sup> F-DCFPyL were expressed more in the peritumoral area than the tumor core, on ex vivo autoradiography (ii) Higher TBR for <sup>18</sup> F-DCFPyL (TBR 6.28-7.92) than <sup>68</sup> Ga-PSMA (TBR 3.22-3.92) on PET (iii) Heterogeneous tissue staining with 3 PSMA antibodies: ab58779 (Abcam) negative ×3, NBP1-45057 (Novus) positive ×3, and NBP1-89822 (Novus) split (iv) Activated astrocyte expression (GFAP) was high peritumorally
Liu et al.	2021	30	14 grade II gliomas 4 grade III gliomas 12 GBMs	Unknown	(i) PSMA-positive IHC staining in 0/14 grade II, 2/4 grade III, and 9/12 grade IV  (i) PSMA expression in all GBMs at initial diagnosis and 15/16 at recurrence (ii) Variable temporal evolution of PSMA expression from diagnosis to recurrence
Holzgreve et al.	2021	16	GBM	Mouse mAb 3E6 (Agilent)	(iii) High vascular PSMA expression at recurrence inversely associated with survival (iv) Increasing PSMA expression over disease course inversely associated with survival (v) No correlation between PSMA expression and MGMT or Ki-67

staining in most GBMs, and among those, the extent of vascular staining was mostly 51-100% and the intensity of staining was mostly moderate or maximum.

Oliveira et al. then produced a preclinical model in which <sup>68</sup>Ga-PSMA and <sup>18</sup>F-DCFPyL binding were studied on ex vivo autoradiography in 38 rats, implanted with either F98, 9L, or U87 glioma cells [23]. They found that both PSMA-targeting tracers exhibited strong binding in the peritumoral area but moderate binding in the tumor core. In vivo animal PET imaging showed a higher tumor to background ratio (TBR) for <sup>18</sup>F-DCFPyL (TBR 6.28-7.92) than <sup>68</sup>Ga-PSMA (TBR 3.22-3.92). Tissue staining with three different anti-PSMA antibodies showed heterogeneous results, with one antibody negative for all three tumor cell lines (ab58779, Abcam), one positive in all three (NBP1-45057, Novus), and one split (NBP1-89822, Novus). PSMA-specific binding was confirmed by application of the PSMA-antagonist PMPA which effectively suppressed <sup>68</sup>Ga-PSMA and <sup>18</sup>F-DCFPyL binding. They found that activated microglia expression (CD11b) was low intratumorally and peritumorally but activated astrocyte expression (GFAP) was high peritumorally. They concluded that PSMA

expression may truly be capturing astrocyte activation instead of tumorigenesis, which would limit its utility in differentiating tumor recurrence from radiation necrosis.

Recently, Liu et al. published a report from 30 glioma patients, in which they demonstrated PSMA expression on IHC staining in zero out of 14 grade II gliomas, two out of four grade III gliomas, and nine out of 12 GBMs [24]. Then, Holzgreve et al. demonstrated, in a series of 16 GBMs, using mouse mAb 3E6 (Agilent), that all 16 had PSMA uptake on IHC at initial diagnosis and 15/16 at recurrence [25]. The change in PSMA expression varied between these time-points, whereas the vessel marker CD34 remained consistent. The level of vascular PSMA expression at recurrence was predictive of survival, as was an increase in PSMA expression over the course of the disease. Notably, PSMA expression was not associated with MGMT status or Ki-67 proliferation index.

In summary, tissue from multiple types of CNS tumors demonstrates PSMA expression. GBM and breast cancer brain metastases tissue showed robust PSMA staining, localized to the neovasculature, with staining present in a majority of cells with moderate to maximum intensity. PSMA



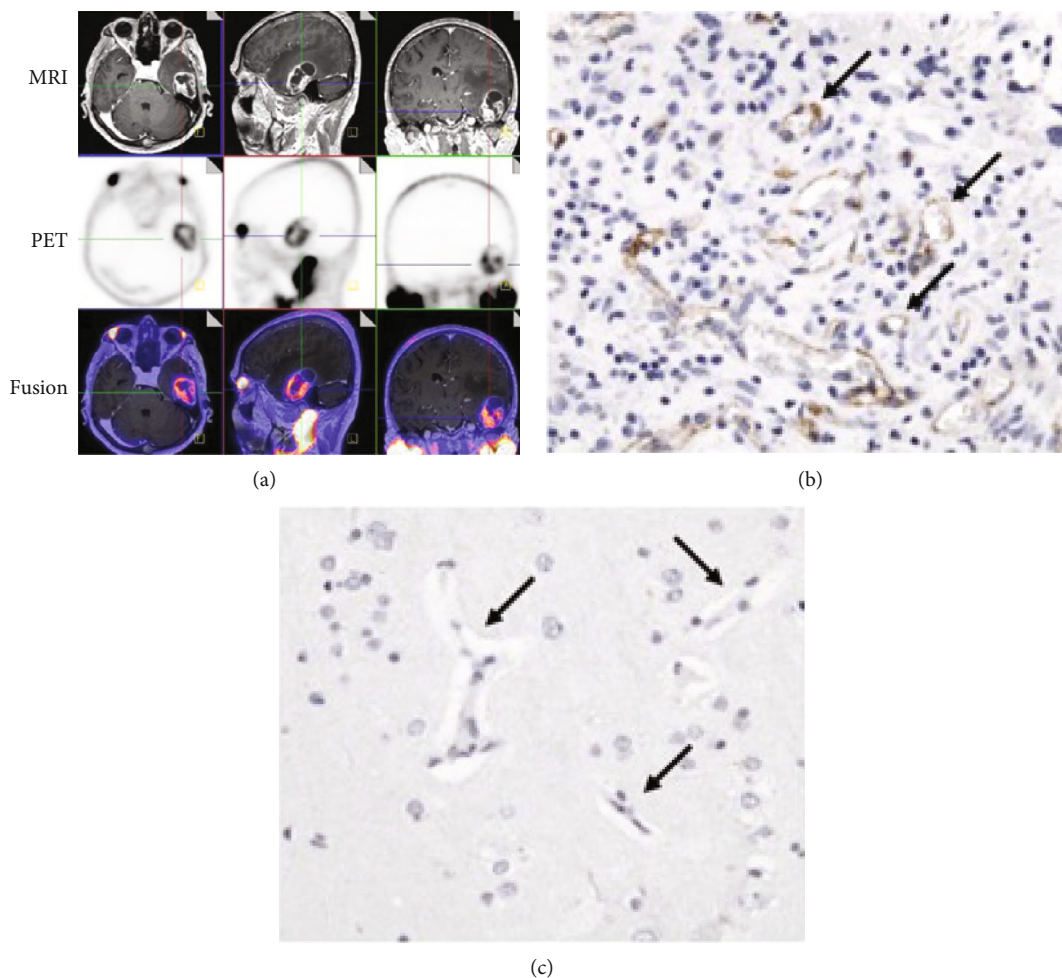


FIGURE 2:  $^{68}\text{Ga}$ -PSMA PET and PSMA immunohistochemistry of representative GBM. (a) MRI,  $^{68}\text{Ga}$ -PSMA PET, and fused images. (b) PSMA expression in GBM vascular endothelium. (c) No PSMA expression in normal brain. Reproduced with permission from Schwenck et al. [17].

staining metrics in GBM were also predictive of survival. Glioma tissue PSMA staining was highly variable across studies. No PSMA staining was seen in radiation necrosis human tissue; however, in glioma cell lines, there was evidence that PSMA expression may capture astrocyte activation instead of tumorigenesis.

**3.2. PSMA-Targeting PET Tracer Properties.** The properties of PSMA-targeting tracers differ on several key features, which results in different strategies for targeting PSMA [26]. For example, some tracers are small-molecule inhibitors while others are monoclonal antibodies [27]. The small-molecule tracers are smaller than antibody tracers and thus can travel faster throughout the vasculature and are excreted faster. Therefore, small-molecule tracers reach more tissue indiscriminately but allow for faster imaging protocols. Antibody tracers travel preferably through larger vessels, which are often seen more in tumor tissue than normal tissue. Therefore, antibody tracers allow for more specific imaging although the scanning protocol is longer. Both of these types of targeting compound are conjugated with a radionuclide to create a radiotracer targeting PSMA.

There is variability between radionuclides, including their half-life and positron range. These tracer characteristics are described in detail below.

**3.2.1. Gallium-Tagged Tracers.** Four formulations of  $^{68}\text{Ga}$ -tagged PSMA-targeting tracer have been developed, including  $^{68}\text{Ga}$ -PSMA-11 (HBED-CC),  $^{68}\text{Ga}$ -PSMA-617,  $^{68}\text{Ga}$ -PSMA-I&T,<sup>28</sup> and  $^{68}\text{Ga}$ -THP-PSMA (Table 2) [28]. The  $^{68}\text{Ga}$  radionuclide is produced in a Ga generator, has a half-life of 1.1 hours, a positron range of 8.9 mm, and is taken up by the bladder wall and kidney [29, 30]. They do not show uptake in normal brain tissue. They may have a lower resolution than other isotopes, due to a longer photon range and the energy within the isotope.

$^{68}\text{Ga}$ -PSMA-11 (HBED-CC) benefits from a high affinity for PSMA-expressing tumors. It also shows rapid blood clearance and lower liver uptake, though it has uptake in salivary glands [29]. PSMA-617 can be labeled with  $^{177}\text{Lu}$ ,  $^{255}\text{Ac}$ , or  $^{90}\text{Y}$ , for theranostic pairing, which gives it the potential to extend beyond the diagnostic sphere and into the treatment of PSMA-expressing lesions.  $^{68}\text{Ga}$ -PSMA-Imaging & Therapy (I&T) has high-affinity tumor uptake

TABLE 2: Summary of PSMA radiotracer properties.

PSMA radiotracer	Compound structure	Radionuclide synthesis	Radionuclide half-life (hours)	Positron range (mm)	Tracer excretion	Critical organ(s)	Brain uptake	Advantages	Disadvantages
<sup>68</sup> Ga-PSMA-11 (HBED-CC) [27, 29]	Small molecule	Ga generator	1.1	8.9	Renal	Bladder wall Kidney	No	(i) High affinity for PSMA-expressing tumors (ii) Rapid blood clearance, low liver uptake	(i) Decreased resolution because of longer photon range (ii) Uptake in salivary glands (i) Decreased resolution because of longer photon range (ii) Uptake in salivary glands
<sup>68</sup> Ga-PSMA-617 <sup>28, 30</sup>	Small molecule	Ga generator	1.1	8.9	Renal	Bladder wall Kidney	No	(i) Potential theranostic pairing with <sup>177</sup> Lu, <sup>255</sup> Ac, or <sup>99</sup> Y	(i) Decreased resolution because of longer photon range (ii) Uptake in salivary glands
<sup>68</sup> Ga-PSMA-I&T <sup>27, 28, 30</sup>	Small molecule	Ga generator	1.1	8.9	Renal	Bladder wall Kidney	No	(i) High affinity for PSMA-expressing tumors (ii) Potential theranostic pairing with <sup>177</sup> Lu or <sup>255</sup> Ac	(i) Decreased resolution because of longer photon range (ii) Uptake in salivary glands
<sup>68</sup> Ga-THP-PSMA [27, 28, 30]	Small molecule	Ga generator	1.1	8.9	Renal	Bladder wall Kidney	No	(i) Production can be done as a one-step process using a kit	(i) Decreased resolution because of longer photon range
<sup>18</sup> F-DCFPyL [27, 30, 31]	Small molecule	Cyclotron	1.8	0.6	Renal	Bladder wall Kidney	No	(i) Better resolution because of shorter photon range (ii) Higher binding affinity for PSMA	(i) Significant salivary gland accumulation
<sup>18</sup> F-PSMA-1007 <sup>27, 30, 31</sup>	Small molecule	Cyclotron	1.8	0.6	Hepatobiliary	Gallbladder Liver	No	(i) Better resolution because of shorter photon range	(i) Significant salivary gland accumulation
<sup>18</sup> F-DCFBC [27, 30, 32]	Small molecule	Cyclotron	1.8	0.6	Renal	Bladder wall Kidney	No	(i) Better resolution because of shorter photon range	(i) Significant salivary gland accumulation (ii) High blood pool activity
<sup>64</sup> Cu-PSMA [27, 33, 36]	Antibody	Cyclotron	12.7	0.6	Biliary	Large intestine Liver Pancreas	No	(i) Potential theranostic pairing with <sup>67</sup> Cu	(i) Low percentage of positron emission
<sup>124</sup> I-MIP-1095 <sup>30, 34</sup>	Small molecule	Cyclotron	100.8	3.4	Hepatobiliary	Kidney Liver Salivary gland	No	(i) Potential theranostic pairing with <sup>131</sup> I	(i) Access to <sup>124</sup> I is challenging

TABLE 2: Continued.

PSMA radiotracer	Compound structure	Radionuclide synthesis	Radionuclide half-life (hours)	Positron range (mm)	Tracer excretion	Critical organ(s)	Brain uptake	Advantages	Disadvantages
<sup>89</sup> Zr-Df-IAB2M [35, 36]	Antibody	Cyclotron	78.4	1.2	Hepatobiliary	Kidney Liver	No	(i) Unknown	(i) Little clinical experience
<sup>99m</sup> Tc-PSMA [37, 87]	Small molecule	Tc generator	6	n/a	Renal	Kidney Liver	No	(i) SPECT more readily available than PET	(i) Little clinical experience (ii) SPECT lesser resolution and less sensitive than PET
<sup>99m</sup> Tc-MIP-1404 [27, 38]	Small molecule	Tc generator	6	n/a	Renal	Kidney Liver Salivary gland	No	(i) SPECT more readily available than PET	(i) Little clinical experience (ii) SPECT lesser resolution and less sensitive than PET
<sup>99m</sup> Tc-MIP-1405 [27, 39]	Small molecule	Tc generator	6	n/a	Renal	Kidney Liver Salivary gland	No	(i) SPECT more readily available than PET	(i) Little clinical experience (ii) SPECT lesser resolution and less sensitive than PET
<sup>99m</sup> Tc-MIP-I&S [40, 87]	Small molecule	Tc generator	6	n/a	Renal Hepatobiliary	Kidney Spleen	No	(i) SPECT more readily available than PET (ii) Potential use in targeted surgery	(i) Little clinical experience (ii) SPECT lesser resolution and less sensitive than PET
<sup>99m</sup> Tc-EDDA/HYNIC-iPSMA [41, 88]	Small molecule	Tc generator	6	n/a	Renal	Kidney Salivary gland	No	(i) SPECT more readily available than PET	(i) Little clinical experience (ii) SPECT lesser resolution and less sensitive than PET

similar to HBED agents and also has theranostic pairing potential, as it can be labeled with <sup>177</sup>Lu or <sup>255</sup>Ac (Table 2). Among these tracers, only <sup>68</sup>Ga-PSMA-11 (HBED-CC) and <sup>68</sup>Ga-THP-PSMA have been studied in CNS tumors to date.

**3.2.2. Fluorine-Tagged Tracers.** Three formulations of <sup>18</sup>F-fluorine- (F-) tagged PSMA-targeting tracers have been developed, including <sup>18</sup>F-DCFpyl [31], <sup>18</sup>F-PSMA-1007 [31], and <sup>18</sup>F-DCFBC [32]. These <sup>18</sup>F radionuclides are produced in a cyclotron, have a half-life of 1.8 hours, a positron range of 0.6 mm, and are not taken up by normal brain tissue

[30–32]. The route of excretion and critical uptake organs vary by tracer, and they include the liver, kidney, bladder wall, and gallbladder. These tracers all benefit from a better resolution than other isotopes, due to their short photon range. However, they all have significant salivary gland uptake.

<sup>18</sup>F-DCFpyl has a higher target-to-background ratio than <sup>68</sup>Ga-PSMA-11 (HBED-CC) and thus may detect more lesions [29]. It has a much higher binding affinity for PSMA than its predecessor, <sup>18</sup>F-DCFBC, which also suffered from high blood pool activity which limited detection of lymph nodes near blood vessels. <sup>18</sup>F-PSMA-1007 is structurally



similar to  $^{68}\text{Ga}$ -PSMA-617 but potentially has a better resolution [31]. When there are low PSA levels, subcentimeter bone lesions, lymph node involvement, or hepatic involvement,  $^{68}\text{Ga}$ -PSMA agents are superior to  $^{18}\text{F}$ -choline (Table 2). Among these, only  $^{18}\text{F}$ -DCFPyl and  $^{18}\text{F}$ -PSMA-1007 have been studied in CNS tumors to date.

**3.2.3. Copper-Tagged Tracers.** One  $^{64}\text{Cu}$  copper- (Cu-) tagged PSMA-targeting tracer was developed, and it was based on the structural base of  $^{68}\text{Ga}$ -PSMA-617 [33]. The  $^{64}\text{Cu}$  radionuclide is produced in a cyclotron, has a long half-life of 12.7 hours, a positron range of 0.6 mm, and accumulates in the liver, large intestine, and pancreas [30, 33]. It is not taken up by normal brain tissue. It benefits from theranostic pairing potential with  $^{67}\text{Cu}$  (Table 2). This radiotracer has not yet been studied in CNS tumors.

**3.2.4. Iodine-Tagged Tracers.** There has been one  $^{124}\text{I}$  iodine- (I-) tagged PSMA-targeting tracer developed,  $^{124}\text{I}$ -MIP-1095 [34]. The  $^{124}\text{I}$  radionuclide is produced in a cyclotron, has a long half-life of 100.8 hours, a positron range of 3.4 mm, and accumulates in the salivary glands, liver, and kidneys [30, 34]. It is not taken up by normal brain tissue. It benefits from theranostic pairing potential with  $^{131}\text{I}$  (Table 2). This radiotracer has not yet been studied in CNS tumors.

**3.2.5. Zirconium-Tagged Tracers.** There has been one  $^{89}\text{Zr}$  zirconium- (Zr-) tagged PSMA-targeting tracer developed,  $^{89}\text{Zr}$ -Df-IAB2M [35]. The  $^{89}\text{Zr}$  radionuclide is produced in a cyclotron, has a long half-life of 78.4 hours, a positron range of 1.2 mm, and accumulates in the liver and kidney [35, 36]. It is not taken up by normal brain tissue. This radiotracer has been studied in CNS tumors, but further clinical investigations are needed to understand its advantages and disadvantages relative to other tracers (Table 2).

**3.2.6. Technetium-Tagged Tracers.** There have been five  $^{99\text{m}}\text{Tc}$  technetium- (Tc-) tagged PSMA-targeting tracers developed, including Tc-PSMA [37], Tc-MIP-1404 [38], Tc-MIP-1405 [39], Tc-PSMA-I&S [40], and Tc-EDDA/HYNIC-iPSMA [41]. These radionuclides are produced by  $^{99\text{m}}\text{Tc}$ -generator and have a half-life of 6 hours [37–41]. The route of excretion and uptake by critical organs varies by tracer, but the kidneys are involved in all five, and none show uptake in normal brain tissue. All five Tc-tagged PSMA-targeting tracers have limited clinical application. As single-photon emission computerized tomography (SPECT) imaging tracers, they have a lower resolution than PET imaging tracers, although SPECT is more readily available in clinical settings than PET. Tc-PSMA-Imaging & Surgery (I&S) is being investigated for potential use in targeted surgery (Table 2). These radiotracers have not been studied in CNS tumors and are unlikely to be developed for this purpose given the superiority of PET over SPECT with regard to resolution.

### 3.3. Diagnostic Performance in Gliomas

**3.3.1. Gallium-PSMA in Gliomas.** Recent years have seen an increase in PSMA-targeting PET imaging studies and case

reports in gliomas, with a total of 20 studies with 122 patients, since 2015 (Table 3). Most of these studies have focused on imaging with the  $^{68}\text{Ga}$ -PSMA radiotracer, though a few have used alternative tracers such as  $^{18}\text{F}$ -DCFPyL,  $^{89}\text{Zr}$ -Df-IAB2M, and  $^{18}\text{F}$ -PSMA-1007. Following the promising results of early immunohistochemistry studies in glioma tissue, the first report of PSMA-targeting PET imaging of a glioma patient was published by Schwenck et al. [17]. They found that  $^{68}\text{Ga}$ -PSMA-11 (HBED-CC) uptake was markedly increased in the contrast-enhancing solid tumor region identified on MRI and that there was no uptake in the normal brain tissue (Figure 2). Then, Unterrainer et al. published the first case report of  $^{68}\text{Ga}$ -PSMA PET imaging in a gliosarcoma patient [18]. They found high  $^{68}\text{Ga}$ -PSMA-11 (HBED-CC) uptake, with a median maximal standardized uptake value ( $\text{SUV}_{\text{max}}$ ) of 3.43 and median maximal TBR ( $\text{TBR}_{\text{max}}$ ) of 48.93.

The first case series of  $^{68}\text{Ga}$ -PSMA PET imaging in GBM was published by Sasikumar et al., which included five GBMs with suspected recurrence and one newly diagnosed GBM [42]. In four out of five GBMs with suspected recurrence, they found increased uptake of both  $^{68}\text{Ga}$ -PSMA-11 (HBED-CC) and  $^{18}\text{F}$ -FDG correlating to the lesion on MRI with histological confirmation. While the uptake of both tracers was spatially correlated, TBR was greater for  $^{68}\text{Ga}$ -PSMA-11 (HBED-CC) (12.9) than for  $^{18}\text{F}$ -FDG (0.96). The 5<sup>th</sup> suspected recurrence, which did not demonstrate uptake with either tracer, did not have recurrence on histology. The newly diagnosed GBM showed intense tracer uptake on the periphery of the lesion, with a TBR of 22.3 for  $^{68}\text{Ga}$ -PSMA-11 (HBED-CC) and 1.11 for  $^{18}\text{F}$ -FDG. In this case series, they noted a better visualization of the lesion using  $^{68}\text{Ga}$ -PSMA-11 (HBED-CC) than  $^{18}\text{F}$ -FDG, which they attribute to its comparatively greater TBR. Sasikumar et al. later published a larger case series of 15 gliomas [43], which included the six GBMs from their 2017 report. In their 2018 report, they found that nine out of 10 suspected recurrences had positive findings on  $^{68}\text{Ga}$ -PSMA-11 (HBED-CC) PET scan, and the one without  $^{68}\text{Ga}$ -PSMA-11 (HBED-CC) uptake had no evidence of recurrence on further testing. The TBR values ranged from 4.07 to 29.4, compared to the patient with no disease whose TBR value was 1.15. They additionally found increased  $^{68}\text{Ga}$ -PSMA-11 (HBED-CC) uptake in two newly diagnosed GBMs and two postsurgical GBMs, but no uptake in a postsurgical grade III oligodendroglioma. Overall, in 13  $^{68}\text{Ga}$ -PSMA-11 (HBED-CC) positive gliomas, the TBR was 34.78 in grade II, 11.9 and 27.0 in grade III, and 4.07–134.8 in grade IV. They concluded that the tracer uptake did not correlate to glioma grade (Figure 3).

A case report from Kunikowska et al. demonstrated high  $^{68}\text{Ga}$ -PSMA uptake in a GBM patient, with a  $\text{SUV}_{\text{max}}$  of 23.7 [44]. A report of  $^{68}\text{Ga}$ -PSMA PET imaging in an oligodendroglioma from Malik et al. [45] demonstrated increased  $^{68}\text{Ga}$ -PSMA uptake in the lesion and better lesion delineation with  $^{68}\text{Ga}$ -PSMA than with  $^{18}\text{F}$ -FDG. Verma et al. published a case series of 10 glioma patients, all of which demonstrated increased uptake on  $^{68}\text{Ga}$ -PSMA-11 (HBED-CC) PET imaging [46]. They found the  $\text{SUV}_{\text{max}}$  among

TABLE 3: Summary of PSMA-targeted imaging in gliomas.

Authors	Year	<i>n</i>	Tumor type	PSMA tracer	Main results
Schwenck et al.	2015	1	GBM	<sup>68</sup> Ga-PSMA	(i) <sup>68</sup> Ga-PSMA uptake corresponded to contrast enhancement on MRI (ii) No <sup>68</sup> Ga-PSMA uptake in unaffected brain regions
Unterrainer et al.	2017	1	Gliosarcoma	<sup>68</sup> Ga-PSMA	(i) High <sup>68</sup> Ga-PSMA uptake, with median SUV <sub>max</sub> 3.43 (range 2.22-5.27) (ii) Median TBR <sub>max</sub> 48.93 (range 31.71-75.29) (i) 4/4 GBMs with confirmed recurrence showed both <sup>68</sup> Ga-PSMA and <sup>18</sup> F-FDG uptake (ii) Higher TBR with <sup>68</sup> Ga-PSMA (12.9) than <sup>18</sup> F-FDG (0.96) in recurrent GBMs
Sasikumar et al.	2017	6*	GBM	<sup>68</sup> Ga-PSMA	(iii) In the newly diagnosed GBM, higher TBR for <sup>68</sup> Ga-PSMA (22.3) than <sup>18</sup> F-FDG (1.11) *These patients were reported again in the Sasikumar (2018) paper (i) 9/9 GBMs with confirmed recurrence showed <sup>68</sup> Ga-PSMA uptake (ii) TBR in recurrent GBM ranged 4.07-29.4, versus 1.15 in patient without recurrence
Sasikumar et al.	2018	15*	Glioma	<sup>68</sup> Ga-PSMA	(iii) Increased <sup>68</sup> Ga-PSMA uptake in newly diagnosed and postsurgical GBM (iv) No <sup>68</sup> Ga-PSMA uptake in postsurgical grade III oligodendroglioma (v) <sup>68</sup> Ga-PSMA uptake does not correlate to glioma grade: 34.78 in grade II, 11.9-27.0 in grade III, 4.07-134.8 in grade IV
Kunikowska et al.	2018	1	GBM	<sup>68</sup> Ga-PSMA	(i) High <sup>68</sup> Ga-PSMA uptake with SUV <sub>max</sub> 23.7
Malik et al.	2018	1	Oligodendroglioma	<sup>68</sup> Ga-PSMA	(i) Better lesion delineation with <sup>68</sup> Ga-PSMA uptake than <sup>18</sup> F-FDG
Verma et al.	2019	10	Glioma	<sup>68</sup> Ga-PSMA	(i) Higher SUV <sub>max</sub> in GBMs (16.93 ± 5.4) than grade II gliomas (2.93 ± 0.3) (ii) Higher TBR in GBMs (13.95) than grade II gliomas (3.42)
Gupta et al.	2020a	1	Recurrent GBM	<sup>68</sup> Ga-PSMA	(i) <sup>68</sup> Ga-PSMA uptake in postoperative cavity
Gupta et al.	2020b	1	GBM with pseudoprogression	<sup>68</sup> Ga-PSMA	(i) Increased <sup>68</sup> Ga-PSMA uptake in this "false positive" (ii) SUV <sub>max</sub> 2.71 (versus 0.52 in normal brain tissue) and TBR 5.21
Kumar et al.	2020	1	Recurrent GBM	<sup>68</sup> Ga-PSMA	(i) <sup>68</sup> Ga-PSMA uptake in MRI-confirmed recurrent lesion (ii) <sup>68</sup> Ga-PSMA uptake decreased with regression of lesion posttherapy
Moreau et al.	2020	1	GBM with pseudoprogression	<sup>68</sup> Ga-PSMA	(i) Increased <sup>68</sup> Ga-PSMA uptake in this "false positive" (ii) SUV <sub>max</sub> 3.2
Pernthaler et al.	2021	1	Oligodendroglioma	<sup>68</sup> Ga-PSMA	(i) Homogenous high <sup>68</sup> Ga-PSMA uptake and <sup>18</sup> F-fluciclovie uptake (ii) Higher SUV <sub>max</sub> with <sup>68</sup> Ga-PSMA (9.7) than <sup>18</sup> F-fluciclovine (6.5)
Pilati et al.	2020	1	GBM	<sup>68</sup> Ga-PSMA	(i) High <sup>68</sup> Ga-PSMA uptake
Zhang et al.	2021	1	Glioma	<sup>68</sup> Ga-PSMA	(i) Heterogeneous <sup>68</sup> Ga-PSMA uptake, lower in the core of the lesion (grade II tissue) and higher in circumferential foci (grade III tissue) (i) 15/15 showed increased <sup>68</sup> Ga-PSMA uptake, which correlated with MRI lesion (ii) Median SUV <sub>max</sub> 6.5 (range 2.1-14.3), SUV <sub>mean</sub> 3.5 (1.3-6.1), TBR 96.7 (range 32.2-357.5)
Kunikowska et al.	2020	15	Recurrent GBM	<sup>68</sup> Ga-PSMA	(i) Moderate correlation between tumor grade and SUV <sub>max</sub> ( $r = 0.53$ ), SUV <sub>mean</sub> ( $r = 0.55$ ), SUV <sub>peak</sub> ( $r = 0.50$ ) (ii) Grade II/III gliomas had significantly lower SUV <sub>max</sub> than GBMs, with a cutoff of 2.3
Akgun et al.	2020	35	Glioma	<sup>68</sup> Ga-PSMA	(iii) LGG versus HGG cutoff for SUV <sub>max</sub> was 1.15 (iv) <sup>68</sup> Ga-PSMA was more sensitive ( $p < 0.0\%$ ) than MRI, but not more specific

TABLE 3: Continued.

Authors	Year	<i>n</i>	Tumor type	PSMA tracer	Main results
Liu et al.	2021	30	Glioma	<sup>68</sup> Ga-PSMA	(v) Ki-67, mitosis, endothelial proliferation, and necrosis were correlated with SUV values, but ATRX mutation was not (i) PSMA PET had higher SUV <sub>max</sub> (0.96) and SUV <sub>mean</sub> (0.94) than FDG PET (0.79, 0.74) (ii) <sup>68</sup> Ga-PSMA PET was more effective for differentiating HGG from LGG
Salas Fragomeni et al.	2017	3	High-grade glioma	<sup>18</sup> F-DCFPyL	(i) <sup>18</sup> F-DCFPyL uptake in 3/3 HGGs, with SUV <sub>max</sub> ranged 5.8-13.5 (ii) No uptake in normal brain tissue
Matsuda et al.	2018	2	High-grade glioma	<sup>89</sup> Zr-Df-IAB2M	(i) In 1, high <sup>89</sup> Zr-Df-IAB2M uptake in contrast-enhancing MRI lesion (ii) In 1, heterogeneous <sup>89</sup> Zr-Df-IAB2M uptake with different distribution than 11C-MET
Marafi et al.	2020	1	Recurrent glioblastoma	<sup>18</sup> F-PSMA	(i) Increased uptake of both <sup>18</sup> F-PSMA and <sup>18</sup> F-FDG in the MRI lesion (ii) Better differentiation with <sup>18</sup> F-PSMA than <sup>18</sup> F-FDG

GBM patients ( $16.93 \pm 5.4$ ) to be significantly higher than that of grade II gliomas ( $2.93 \pm 0.3$ ), as well as the TBR ( $13.95$  versus  $3.42$ ), which runs contrary to the results of the Sasikumar et al. (2018) report.

Gupta et al. published a report of a recurrent GBM with <sup>68</sup>Ga-PSMA-11 (HBED-CC) PET scan in the immediate postoperative period, which demonstrated residual <sup>68</sup>Ga-PSMA-11 (HBED-CC) uptake in the margin of the postoperative cavity [47]. Gupta et al. (2020b) also published a report of increased <sup>68</sup>Ga-PSMA-11 (HBED-CC) uptake on PET imaging of a posttreatment GBM with suspected recurrence, which was ultimately diagnosed as pseudoprogression based on subsequent imaging. The lesion SUV<sub>max</sub> was 2.71, versus 0.52 in normal brain, and a TBR of 5.21. They warn that this false positive indicates that <sup>68</sup>Ga-PSMA may not be fully able to differentiate recurrence from radiation necrosis. Moreau et al. echoed these concerns in their case report of a GBM patient with modest <sup>68</sup>Ga-PSMA-11 (HBED-CC) uptake (SUV<sub>max</sub> of 3.2), who was determined to have post-radiation changes based on clinical imaging [48]. Without an established threshold for defining recurrence versus post-radiation effect, it may be difficult to interpret some of the <sup>68</sup>Ga-PSMA PET images, especially given the wide range of values for SUV<sub>max</sub> and TBR that have thus far been demonstrated in gliomas.

Pernthaler et al. report an oligodendroglioma patient with homogeneously high <sup>68</sup>Ga-PSMA-11 (HBED-CC) uptake and <sup>18</sup>F-fluciclovine uptake, on PET imaging [49]. The SUV<sub>max</sub> of <sup>68</sup>Ga-PSMA-11 (HBED-CC) (9.7) was greater than that of <sup>18</sup>F-fluciclovine (6.5). Pilati et al. reported another case of GBM with high <sup>68</sup>Ga-PSMA-11 (HBED-CC) uptake on PET imaging [50]. Kumar et al. report a case of recurrent GBM with high <sup>68</sup>Ga-PSMA-11 (HBED-CC) uptake on PET, which decreased as the tumor regressed posttherapy [51]. Zhang et al. (2020) report a glioma patient with heterogeneous <sup>68</sup>Ga-PSMA uptake which was low in the core of the lesion and higher within foci along the edge of the lesion. On histopathology, it was found that

the low uptake areas were grade II glioma tissue while the high uptake areas were grade III glioma tissue [52].

Kunikowska et al. published the largest series of GBMs imaged with <sup>68</sup>Ga-PSMA-11 (HBED-CC) PET ( $n = 15$ ) [53]. They found 100% spatial correlation of <sup>68</sup>Ga-PSMA-11 (HBED-CC) uptake with MRI lesions, and 100% of the patients demonstrated increased <sup>68</sup>Ga-PSMA-11 (HBED-CC) uptake, though the intensities and patterns differed. The median SUV<sub>max</sub> was 6.5 (range 2.1-14.3), SUV<sub>mean</sub> was 3.5 (range 1.3-6.1), and TBR was 96.7 (range 32.2-357.5). This TBR range is higher even than the range reported by Sasikumar et al. [43] which indicates a high degree of differentiation between tumor and normal brain. These values are also higher than the reported TBRs of amino acid PET tracers like <sup>18</sup>F-FET and <sup>11</sup>C-MET PET [54], which demonstrates that <sup>68</sup>Ga-PSMA better differentiates lesions from the background. Kunikowska et al. also investigated the tumor-to-liver (TLR) ratio because a TLR of 1.5 or higher is needed to be eligible for current PSMA-based radionuclide targeted therapy. They found the median TLR was 0.8 (range 0.6-1.8), and only 2/15 (13%) patients had a TLR of 1.5 or higher.

The largest glioma case series imaged with <sup>68</sup>Ga-PSMA PET ( $n = 35$ ) was published by Akgun et al., in which they found tumor grade to be moderately correlated with SUV<sub>max</sub> ( $r = 0.53$ ), SUV<sub>mean</sub> ( $r = 0.55$ ), and SUV<sub>peak</sub> ( $r = 0.50$ ) [55]. Grade II and III glioma SUV values were each significantly different from grade IV gliomas, though grade II and III were not significantly different from each other. To differentiate grade II/III from grade IV, the SUV<sub>max</sub> cutoff was 2.3 (sensitivity 80%, specificity 81.8%, PPV 81.5%, NPV 80.3%). To differentiate low-grade glioma (LGG; grade II) from high-grade glioma (HGG; grades III/IV), the SUV<sub>max</sub> cutoff was 1.15 (sensitivity 85.7%, specificity 85.7%, PPV 85.7%, NPV 85.7%), which compared favorably to MRI (sensitivity 71.4%, specificity 85.4%) in diagnosing HGG. <sup>68</sup>Ga-PSMA PET was significantly more sensitive ( $p < 0.05$ ) than MRI, but not more specific. They also found that Ki-

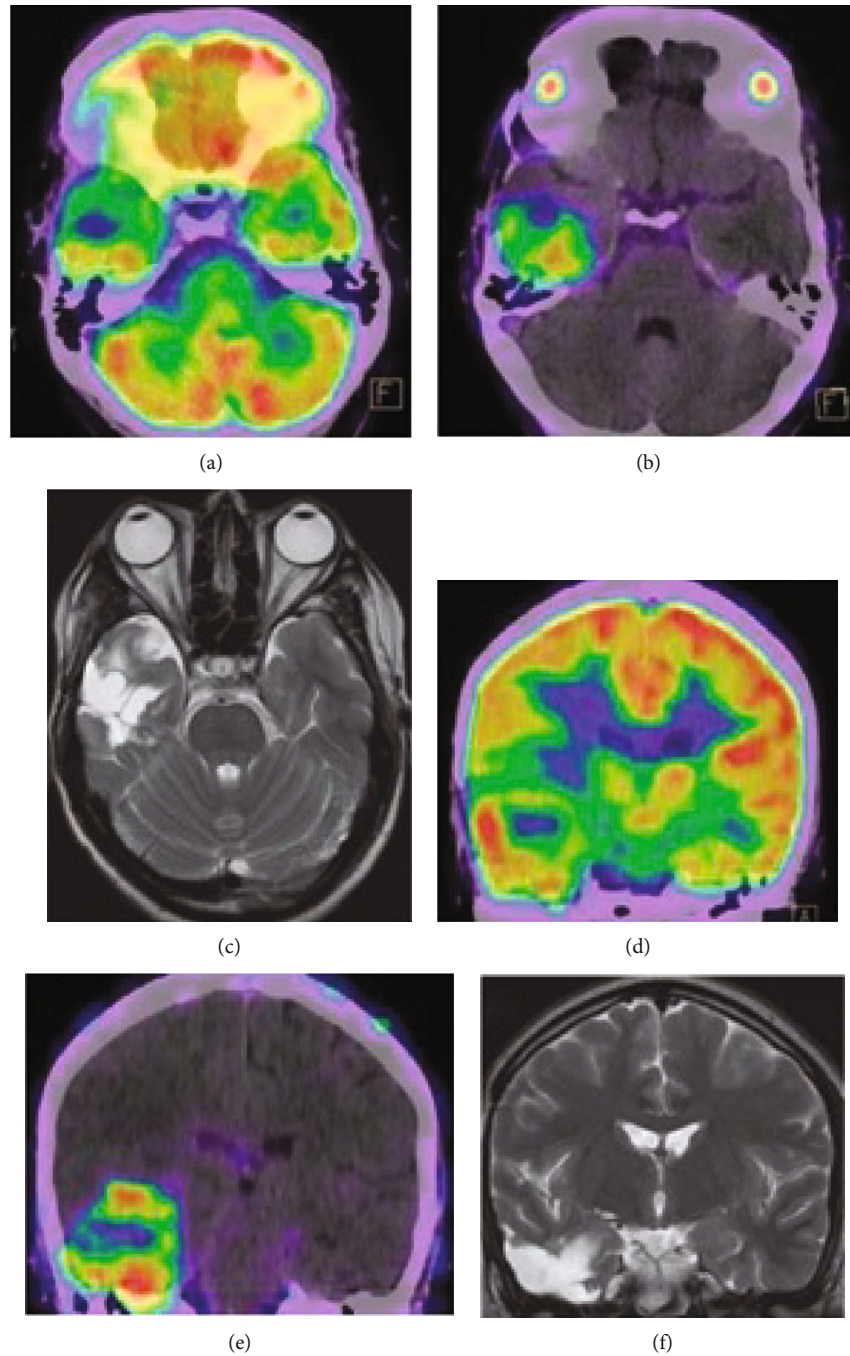


FIGURE 3:  $^{18}\text{F}$ -FDG and  $^{68}\text{Ga}$ -PSMA PET imaging of representative GBM. (a) Axial  $^{18}\text{F}$ -FDG PET/CT. (b) Axial  $^{68}\text{Ga}$ -PSMA-11 PET/CT. (c) Axial T2-weighted MRI. (d) Coronal  $^{18}\text{F}$ -FDG PET/CT. (e) Coronal  $^{68}\text{Ga}$ -PSMA-11 PET/CT. (f) Coronal T2-weighted MRI. Reproduced with permission from Figure 1 in Sasikumar et al. [42].

67, an immunohistochemical proliferation index, was moderately correlated with  $\text{SUV}_{\text{max}}$  ( $r = 0.51$ ),  $\text{SUV}_{\text{mean}}$  ( $r = 0.48$ ), and  $\text{SUV}_{\text{peak}}$  ( $r = 0.44$ ). Mitosis was highly correlated with  $\text{SUV}_{\text{max}}$  ( $r = 0.64$ ) and moderately correlated with  $\text{SUV}_{\text{mean}}$  ( $r = 0.58$ ) and  $\text{SUV}_{\text{peak}}$  ( $r = 0.56$ ). Endothelial proliferation was moderately correlated with  $\text{SUV}_{\text{mean}}$  ( $r = 0.40$ ). Necrosis was moderately correlated with  $\text{SUV}_{\text{max}}$  ( $r = 0.48$ ),  $\text{SUV}_{\text{mean}}$  ( $r = 0.56$ ), and  $\text{SUV}_{\text{peak}}$  ( $r = 0.49$ ). ATRX mutation status was not significantly correlated to any SUV value.

In a study of 30 pathology-confirmed glioma patients, Liu et al. found that  $\text{SUV}_{\text{max}}$  and  $\text{SUV}_{\text{mean}}$  were higher for  $^{68}\text{Ga}$ -PSMA PET (AUC 0.96 and 0.94) than for FDG PET (AUC 0.79, 0.74) [24].  $^{68}\text{Ga}$ -PSMA PET was more effective than FDG PET for distinguishing HGG from LGG.  $^{68}\text{Ga}$ -PSMA  $\text{SUV}_{\text{max}}$  for LGG was 0.74 and for HGG was 5.8, while FDG  $\text{SUV}_{\text{max}}$  was 9.2 for LGG and 11.8 for HGG. With a cutoff of 2.21,  $^{68}\text{Ga}$ -PSMA  $\text{SUV}_{\text{max}}$  achieved sensitivity 0.81, specificity 1.00, and  $p < 0.001$ , while with a cutoff of



10.41, FDG  $SUV_{max}$  achieved sensitivity 0.69, specificity 0.86, and  $p = 0.0083$ .

3.3.2.  $^{18}F$ -DCFPyL,  $^{89}Zr$ -Df-IAB2M, and  $^{18}F$ -PSMA-1007 in Gliomas. Although most PSMA-targeting PET imaging studies in glioma have been done with the  $^{68}Ga$ -PSMA tracer, there have been a few studies with alternate tracers. Salas Fragomeni et al. evaluated  $^{18}F$ -DCFPyL PET in 3 HGGs, which all showed increased  $^{18}F$ -DCFPyL uptake [19]. The  $SUV_{max}$  ranged from 5.8 to 13.5 in tumor lesions, and no uptake was seen in normal brain tissue. Matsuda et al. used  $^{89}Zr$ -Df-IAB2M PET to image 2 HGGs [20]. One HGG showed high uptake in the areas of robust contrast enhancement and low uptake in the areas of lesser enhancement. The other HGG showed high but heterogeneous uptake within the lesion, but with a different distribution pattern than  $^{11}C$ -MET uptake. Marafi et al. evaluated 1 recurrent GBM patient with  $^{18}F$ -PSMA-1007 PET [56]. This patient showed increased uptake of both  $^{18}F$ -PSMA-1007 and  $^{18}F$ -FDG in the area of the lesion on MRI, though the differential uptake of  $^{18}F$ -PSMA-1007 in tumor versus normal brain was better than  $^{18}F$ -FDG, so the lesion was more clearly delineated with  $^{18}F$ -PSMA-1007.

3.3.3. PSMA in Gliomas Summary. In summary,  $^{68}Ga$ -tagged PSMA-targeting PET showed robust uptake in gliomas and GBMs, with no uptake in normal brain regions. Across glioma grades, these tracers showed greater uptake than  $^{18}F$ -FDG. There is conflicting data about whether these uptake values are correlated with tumor grade, but  $SUV_{max}$  cutoff of 2.3 has been proposed for differentiating grade II/III and IV gliomas and  $SUV_{max}$  1.15 or 2.21 for LGG and HGG. Radiation necrosis also demonstrated increased uptake, which calls into question whether this imaging modality can be used to differentiate progression from pseudoprogression. Little research has been done on  $^{18}F$ - and  $^{89}Zr$ -tagged PSMA-targeting tracers.

#### 3.4. Diagnostic Performance in Nonglioma CNS Tumors

3.4.1. Brain Metastases from Prostate Cancer. Metastases to the brain from prostate cancer are rare, with few reported cases in the literature. There are 10 published case reports ( $n = 18$  patients) of  $^{68}Ga$ -PSMA PET imaging of such metastases (Table 4). In nearly all cases, these were detected incidentally on  $^{68}Ga$ -PSMA screening for metastases.

In some reports, the diagnosis of prostate cancer metastasis was made using MRI. The first was published in 2015 by Chakraborty et al., in which they reported a prostatic adenocarcinoma patient without neurologic symptoms, who demonstrated avid  $^{68}Ga$ -PSMA-11 (HBED-CC) uptake in three separate MRI-diagnosed brain metastases, in the cerebellar hemisphere and bifrontal lobes [57]. Dureja et al. reported a prostate adenocarcinoma patient without neurologic symptoms who was found on  $^{68}Ga$ -PSMA-11 (HBED-CC) PET imaging to have at least four MRI-diagnosed brain metastases in the frontal and frontoparietal lobes [58]. The  $SUV_{max}$  of the largest lesion was 4.0. Langsteger et al. reported the only MRI-diagnosed spinal cord metastasis from prostate cancer detected with  $^{68}Ga$ -PSMA PET imag-

ing [59]. The patient had no neurologic symptoms but was found to have  $^{68}Ga$ -PSMA uptake in the spinal cord at the T4-T10 levels.

In other reports, the diagnosis was confirmed by histopathology. Chan et al. reported a patient with prostate cancer who presented with mild ataxia and nausea and upon imaging with  $^{68}Ga$ -PSMA-11 (HBED-CC) was found to have a single metastasis in the cerebellum [60]. The  $^{68}Ga$ -PSMA-11 (HBED-CC) uptake in the lesion was  $SUV_{max}$  5.9, and diagnosis was confirmed by histopathology consistent with high-grade metastatic prostate adenocarcinoma with positive staining for PSMA. Ross et al. reported an asymptomatic temporal lobe metastasis which was not detected on conventional imaging, but was found on  $^{68}Ga$ -THP-PSMA PET imaging and was confirmed with histopathology to be prostate adenocarcinoma [61]. Yin et al. (2019) reported a patient with prostate adenocarcinoma without neurologic symptoms who was found incidentally to have temporal and occipital metastatic lesions on  $^{68}Ga$ -PSMA PET [62]. The lesions demonstrated  $^{68}Ga$ -PSMA avidity with  $SUV_{max}$  ranging 3-11, and not all of the metastases were detected on MRI. Histopathology confirmed the diagnosis and demonstrated positive staining for PSA. Of note, this is reported to be the longest surviving prostate cancer patient with multiple brain metastases at three years, which the authors attribute to the early detection with  $^{68}Ga$ -PSMA PET.

In two reports, the application of PSMA therapeutics reduced both the size of the metastases and the  $^{68}Ga$ -PSMA uptake on PET imaging. Wei et al. reported two prostate cancer patients with known brain metastases who underwent  $^{68}Ga$ -PSMA-11 (HBED-CC) PET imaging for restaging and demonstrated distinct  $^{68}Ga$ -PSMA-11 (HBED-CC) uptake in the cerebral lesions [63]. The  $^{68}Ga$ -PSMA-11 (HBED-CC) uptake in these two patients decreased as the size of the lesions regressed, following combined  $^{177}Lu$ -PSMA-617 with radiotherapy. Sathegke et al. reported one castration-resistant prostate cancer patient with several cerebral metastases that showed avid  $^{68}Ga$ -PSMA uptake on PET imaging [64]. Following treatment with  $^{225}Ac$ -PSMA-617, the size and  $^{68}Ga$ -PSMA uptake of the cerebral metastases decreased, along with the PSA levels. On the other hand, Parihar et al. reported a case of new brain metastases with  $^{68}Ga$ -PSMA uptake, after treatment of prostate cancer with  $^{177}Lu$ -PSMA and  $^{225}Ac$ -PSMA [65]. This patient was treated with docetaxel, cabazitaxel, enzalutamide, and two cycles of  $^{177}Lu$ -PSMA therapy, and then four cycles of  $^{225}Ac$ -PSMA therapy. After two cycles of  $^{225}Ac$ -PSMA therapy,  $^{68}Ga$ -PSMA PET/CT imaging did not demonstrate any brain lesion, and then after four total cycles of  $^{225}Ac$ -PSMA, imaging revealed new brain lesions in the setting of generalized disease progression.

The first extended case series of PSMA-targeting PET in prostate cancer brain metastasis ( $n=8$ ), by McBean et al., revealed considerable variability across patients [66]. Only three out of eight patients presented with neurological symptoms, and the  $^{68}Ga$ -PSMA avidity ranged from not avid to intense, while the  $SUV_{max}$  ranged from 2 to 21. Of note, four out of eight patients had previously undergone  $^{177}Lu$ -PSMA therapy for their primary prostate cancer, but



TABLE 4: Summary of PSMA-targeted imaging in prostate cancer brain metastases.

Authors	Year	<i>n</i>	PSMA tracer	Main results
Chakraborty et al.	2015	1	<sup>68</sup> Ga-PSMA	(i) Asymptomatic, avid <sup>68</sup> Ga-PSMA uptake in 3 separate brain metastases, confirmed by MRI
Dureja et al.	2017	1	<sup>68</sup> Ga-PSMA	(i) Asymptomatic, <sup>68</sup> Ga-PSMA uptake in 4 brain metastases (SUV <sub>max</sub> 4.0), confirmed by MRI
Langsteger et al.	2017	1	<sup>68</sup> Ga-PSMA	(i) Asymptomatic, <sup>68</sup> Ga-PSMA uptake in T4-T10 spinal cord metastases, confirmed by MRI
Chan et al.	2017	1	<sup>68</sup> Ga-PSMA	(i) Symptomatic, <sup>68</sup> Ga-PSMA uptake in single cerebellar metastasis (SUV <sub>max</sub> 5.9), confirmed by pathology
Ross et al.	2020	1	<sup>68</sup> Ga-PSMA	(i) Asymptomatic, single brain metastasis detected with <sup>68</sup> Ga-PSMA but not with standard imaging, confirmed by pathology
Yin et al.	2019	1	<sup>68</sup> Ga-PSMA	(i) Asymptomatic, <sup>68</sup> Ga-PSMA uptake in multiple brain metastases (SUV <sub>max</sub> 3-11) and not all detected on MRI, confirmed by pathology
Wei et al.	2017	2	<sup>68</sup> Ga-PSMA	(i) Distinct <sup>68</sup> Ga-PSMA uptake in cerebral metastases (ii) Decreased uptake as lesion regressed posttherapy
Sathekge et al.	2019	1	<sup>68</sup> Ga-PSMA	(i) Several cerebral metastases avidly showed <sup>68</sup> Ga-PSMA uptake (ii) Size and <sup>68</sup> Ga-PSMA uptake decreased posttherapy
McBean et al.	2021	8	<sup>68</sup> Ga-PSMA	(i) 3/8 presented with neurological symptoms (ii) 4/8 had previously undergone <sup>177</sup> Lu-PSMA therapy (iii) PSMA avidity ranged from not avid to intense, and SUV <sub>max</sub> ranged 2-21
Parihar et al.	2021	1	<sup>68</sup> Ga-PSMA	(i) <sup>68</sup> Ga-PSMA uptake in new brain metastases, after <sup>177</sup> Lu-PSMA and <sup>225</sup> Ac-PSMA therapy

TABLE 5: Summary of PSMA-targeted imaging in nonprostate cancer brain metastases.

Authors	Year	<i>n</i>	Primary lesion	PSMA tracer	Main results
Medina-Ornelas et al.	2017	1	Breast	<sup>68</sup> Ga-PSMA	(i) Symptomatic, brain metastasis showed <sup>68</sup> Ga-PSMA uptake, confirmed by pathology
Malik et al.	2018	1	Breast	<sup>68</sup> Ga-PSMA	(i) Cerebella metastasis avidly showed <sup>68</sup> Ga-PSMA uptake but not FDG
Marafi et al.	2020	1	Breast	<sup>68</sup> Ga-PSMA	(i) Intense <sup>68</sup> Ga-PSMA uptake in cerebral and cerebella metastases, confirmed by MRI (ii) No uptake in normal brain tissue
Arslan et al.	2021	1	Breast	<sup>68</sup> Ga-PSMA	(i) Avid <sup>68</sup> Ga-PSMA uptake but low FDG uptake in recurrent brain metastasis, confirmed by pathology
Rowe et al.	2015	1	Kidney	<sup>18</sup> F-DCFPyL	(i) Intense <sup>18</sup> F-DCFPyL uptake in brain metastasis (SUV <sub>max</sub> 3.9), confirmed by MRI
Yin et al.	2019	1	Kidney	<sup>18</sup> F-DCFPyL	(i) <sup>18</sup> F-DCFPyL uptake in 3 brain metastases (SUV <sub>max</sub> 0.5-3.4), confirmed by imaging
Hod et al.	2017	1	Melanoma	<sup>68</sup> Ga-PSMA	(i) Unexpected avid <sup>68</sup> Ga-PSMA uptake in brain metastasis, confirmed by pathology
Matsuda et al.	2018	1	Lung	<sup>89</sup> Zr-Df-IAB2M	(i) Avid <sup>89</sup> Zr-Df-IAB2M uptake corresponding to MRI lesion, confirmed by pathology (ii) No uptake in normal brain tissue

this did not correlate with any trends in their imaging findings.

**3.4.2. Brain Metastases from Nonprostate Cancer.** There has also been a selection of case reports of brain metastases that arise from nonprostate cancers that nevertheless demon-

strate significant PSMA-targeted tracer uptake on PET (Table 5). Four such reports of PSMA-ligand uptake in brain metastases from breast cancer patients have been published. Medina-Ornelas et al. reported a patient with HER-2-positive breast carcinoma, who presented with progressive headache and dizziness, and was subsequently found to have

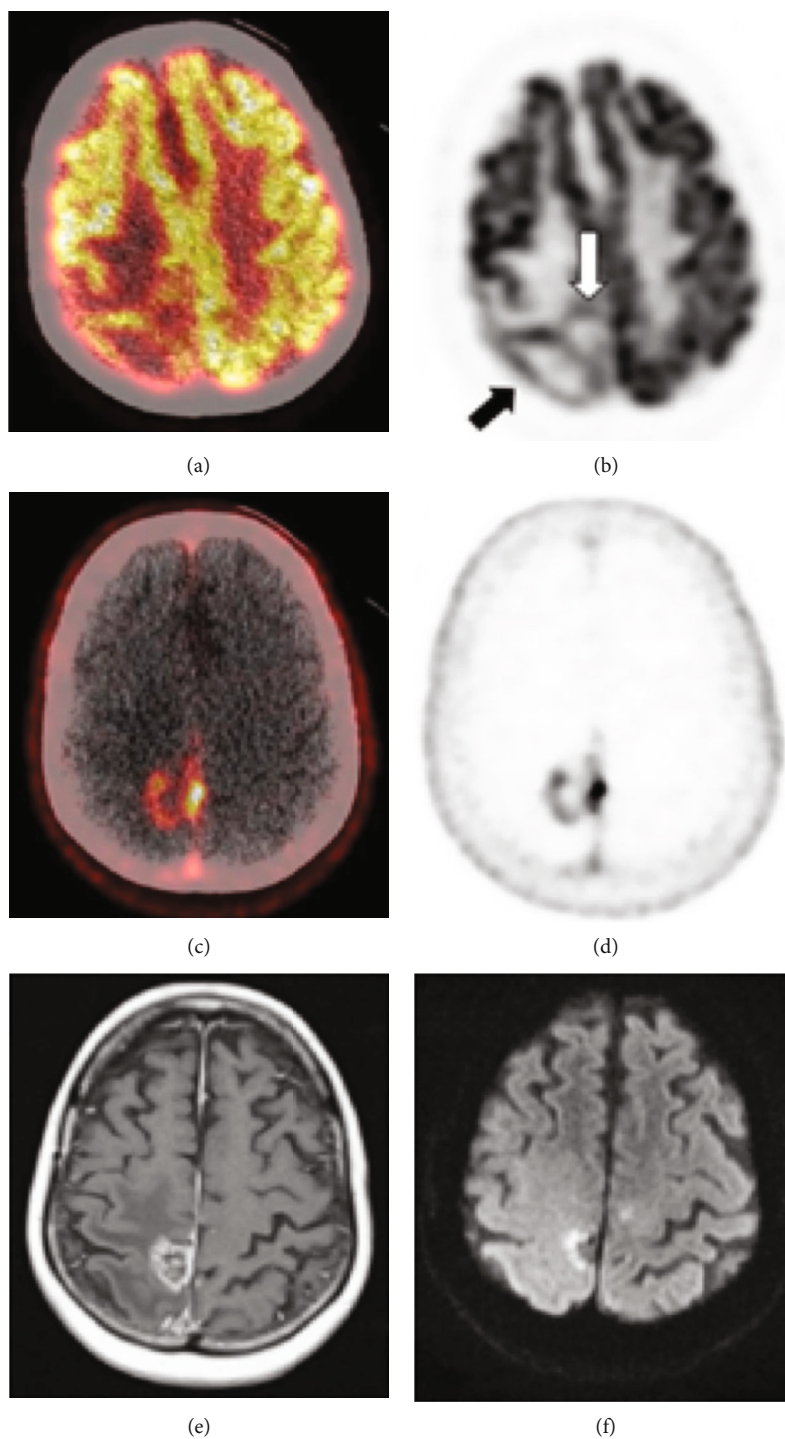


FIGURE 4:  $^{18}\text{F}$ -FDG and  $^{18}\text{F}$ -PSMA PET MRI imaging of representative breast cancer brain metastasis. (a)  $^{18}\text{F}$ -FDG PET/CT. (b)  $^{18}\text{F}$ -FDG PET. (c)  $^{18}\text{F}$ -PSMA-1007 PET/CT. (d)  $^{18}\text{F}$ -PSMA-1007 PET. (e) T1-weighted MRI. (f) DWI MRI. Reproduced with permission from Figure 1 in Marafi et al. [68].

a supratentorial brain metastasis on MRI and  $^{68}\text{Ga}$ -PSMA PET, confirmed by histopathology [67]. Malik et al. reported a breast cancer patient with a cerebellar brain metastasis that avidly accumulated  $^{68}\text{Ga}$ -PSMA, but not  $^{18}\text{F}$ -FDG [45]. Marafi et al. also reported a breast cancer patient with intense  $^{18}\text{F}$ -PSMA-1007 uptake in several MRI-diagnosed metastases in the parietal lobe and cerebellum, without

uptake in normal tissue (Figure 4) [68]. Arslan et al. reported a triple-negative breast cancer patient with a recurrent brain metastasis that demonstrated avid  $^{68}\text{Ga}$ -PSMA-11 (HBED-CC) uptake, but low FDG [69]. Diagnosis of this frontoparietal lesion was confirmed by histopathology.

Two reports have been published of  $^{18}\text{F}$ -DCFPyL uptake on PET in metastatic renal cell carcinomas (RCC), one clear

TABLE 6: Summary of PSMA-targeted imaging in meningiomas.

Authors	Year	<i>n</i>	PSMA tracer	Main results
Bilgin et al.	2016	1	<sup>68</sup> Ga-PSMA	(i) High <sup>68</sup> Ga-PSMA uptake in brain lesion (SUV <sub>max</sub> 3.1), diagnosed as meningioma on MRI
Jain et al.	2017	1	<sup>68</sup> Ga-PSMA	(i) Avid <sup>68</sup> Ga-PSMA uptake in meningioma (SUV <sub>max</sub> 1.9) but no FDG avidity
Sasikumar et al.	2017	1	<sup>68</sup> Ga-PSMA	(i) Stronger <sup>68</sup> Ga-PSMA uptake (SUV <sub>max</sub> 14.6, TBR 29.2) than FDG (SUV <sub>max</sub> 6.44, TBR 0.74) (ii) Meningioma diagnosis confirmed by pathology
Gupta et al.	2020	1	<sup>68</sup> Ga-PSMA	(i) Avid <sup>68</sup> Ga-PSMA uptake, diagnosis confirmed by MRI
Courtney et al.	2021	1	<sup>68</sup> Ga-PSMA	(i) <sup>68</sup> Ga-PSMA uptake demonstrated in a meningioma
Junqueira et al.	2021	1	<sup>68</sup> Ga-PSMA	(i) Strong <sup>68</sup> Ga-PSMA uptake demonstrated in an intraventricular meningioma (SUV <sub>max</sub> 12.1)
Calabria et al.	2017	1	<sup>64</sup> Cu-PSMA	(i) <sup>64</sup> Cu-PSMA uptake in MRI-confirmed meningioma was SUV <sub>max</sub> 3.8 at 1 h postinjection, 3.9 at 4 h postinjection
Haemels et al.	2020	1	<sup>18</sup> F-PSMA	(i) Moderately avid <sup>18</sup> F-PSMA uptake in pathology-confirmed meningioma

cell and one nonclear cell. Rowe et al. reported a clear cell RCC patient who demonstrated intense <sup>18</sup>F-DCFPyL uptake in an MRI-diagnosed frontal lobe brain metastasis (SUV<sub>max</sub> = 3.9) [70]. Yin et al. reported a nonclear cell RCC patient with three CT-diagnosed brain metastases, in the parietal and temporal lobes, with <sup>18</sup>F-DCFPyL SUV<sub>max</sub> ranging from 0.5 to 3.4 [71].

There is only one report of <sup>68</sup>Ga-PSMA uptake in a brain metastasis from melanoma. Hod et al. reported a patient who demonstrated a melanoma metastasis in the occipital lobe on CT and MRI and unexpectedly showed avid <sup>68</sup>Ga-PSMA uptake in the lesion [72]. Diagnosis was confirmed by histopathology.

Similarly, there has been only one report of <sup>89</sup>Zr-Df-IAB2M uptake in brain metastases from lung cancer. Matsuda et al. report a lung cancer patient with MRI-detected occipital brain metastasis, which demonstrated avid <sup>89</sup>Zr-Df-IAB2M uptake [20]. There was no uptake in normal tissue. Diagnosis was confirmed by histopathology, and immunohistochemical analysis demonstrated a trend toward a positive correlation between <sup>89</sup>Zr-Df-IAB2M uptake and PSMA expression.

**3.4.3. Meningiomas.** PSMA targeting is potentially well suited to meningiomas, given that these lesions are generally highly vascularized. There have been eight single case reports published of PSMA-targeted PET imaging in meningioma patients, all of which were incidental findings in patients with prostate cancer (Table 6). Often the lesions were suspected brain metastases that were ultimately diagnosed as meningiomas. In six of these reports, the PSMA-binding tracer utilized was <sup>68</sup>Ga-PSMA. Bilgin et al. reported a patient with high <sup>68</sup>Ga-PSMA uptake in an orbitofrontal lesion (SUV<sub>max</sub> = 3.1) which was subsequently diagnosed as meningioma on MRI [73] (Figure 5). Another report, by Jain et al., found that a frontal convexity meningioma demonstrated avid <sup>68</sup>Ga-PSMA uptake

(SUV<sub>max</sub> = 1.9), but no FDG avidity [74]. Sasikumar et al. reported a patient with an ambiguous lesion on MRI, which demonstrated stronger <sup>68</sup>Ga-PSMA-11 (HBED-CC) uptake (SUV<sub>max</sub> lesion 14.6, SUV<sub>max</sub> background 0.5, TBR 29.2) than <sup>18</sup>F-FDG uptake (SUV<sub>max</sub> lesion 6.44, SUV<sub>max</sub> background 8.62, TBR 0.74) [42]. Histopathology confirmed a diagnosis of atypical meningioma. Gupta et al. also reported a parietal lobe meningioma that demonstrated avid <sup>68</sup>Ga-PSMA uptake, and diagnosis was supported by MRI [75]. Courtney et al. reported a patient with a history of prostate cancer who demonstrated <sup>68</sup>Ga-PSMA uptake in the left frontal lobe, confirmed as a preexisting meningioma [76]. Finally, Junqueira et al. reported avid <sup>68</sup>Ga-PSMA uptake (SUV<sub>max</sub> 12.1) in an MRI-detected lesion, suggestive of an intraventricular meningioma of a patient with history of prostate cancer [77].

One report utilized the <sup>64</sup>Cu-PSMA tracer. Calabria et al. reported an MRI-detected foramen magnum meningioma with SUV<sub>max</sub> of 3.8 at 1 hour after tracer administration and 3.9 at four hours postadministration [78].

Similarly, one report utilized the <sup>18</sup>F-PSMA-1007 tracer. Haemels et al. reported a patient with moderately avid <sup>18</sup>F-PSMA-1007 uptake in the occipital lobe [79]. This was diagnosed by histopathology as a transitional-type meningioma. Tissue autoradiography studies revealed specific <sup>18</sup>F-PSMA-1007 binding, which could be inhibited by 2-PMPA.

**3.4.4. Other CNS Tumors.** There are an additional three case reports (with *n* = 4 patients) of <sup>68</sup>Ga-PSMA PET imaging in other CNS tumors, including CNS lymphoma, intracranial hemangiopericytoma, and hemangioblastoma. Sasikumar et al. reported two patients with histopathology-confirmed CNS lymphoma [42]. They both demonstrated higher <sup>68</sup>Ga-PSMA-11 (HBED-CC) uptake than <sup>18</sup>F-FDG uptake: in the first patient, <sup>68</sup>Ga-PSMA-11 (HBED-CC) uptake showed TBR of 17.0 (SUV<sub>max</sub> lesion 3.07, SUV<sub>max</sub> background 0.18), and <sup>18</sup>F-FDG uptake showed TBR 4.85

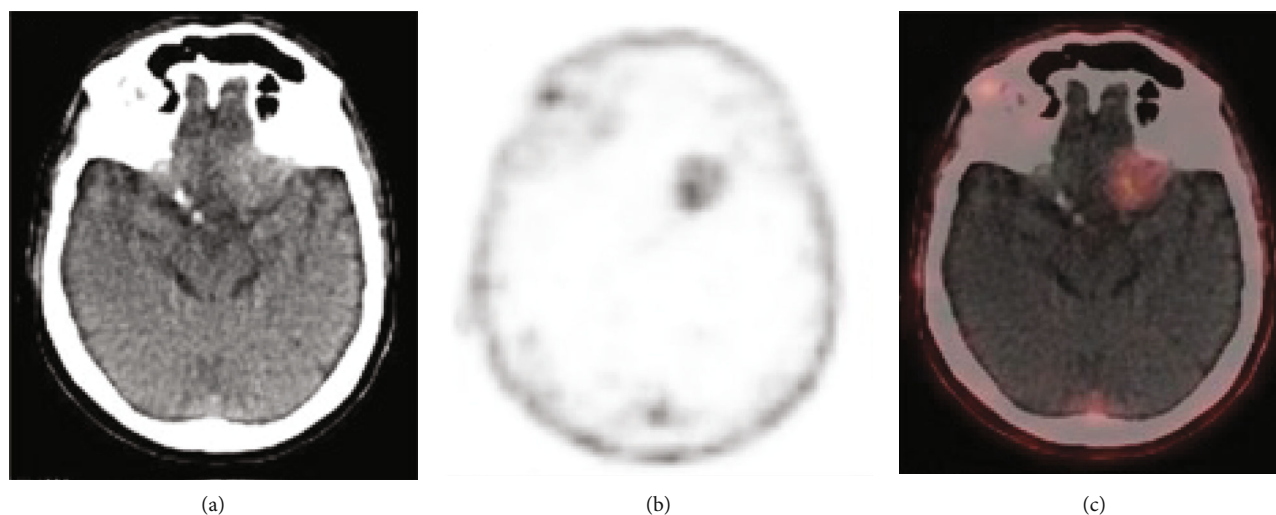


FIGURE 5:  $^{68}\text{Ga}$ -PSMA PET/CT in a representative meningioma. (a) T1-weighted MRI. (b) Head CT. (c)  $^{68}\text{Ga}$ -PSMA PET/CT. Reproduced with permission from Figure 2 of Bilgin et al. [73].

( $\text{SUV}_{\max}$  lesion 28.7,  $\text{SUV}_{\max}$  background 5.91, TBR); in the second,  $^{68}\text{Ga}$ -PSMA-11 (HBED-CC) uptake showed TBR of 37.2, versus 3.6 for  $^{18}\text{F}$ -FDG. Patro et al. reported a patient with an intracranial hemangiopericytoma in the posterior fossa, which demonstrated intense  $^{68}\text{Ga}$ -PSMA-11 (HBED-CC) uptake and mild  $^{18}\text{F}$ -FDG enhancement [80]. Gohimont et al. reported a patient with a history of prostate cancer, who demonstrated  $^{68}\text{Ga}$ -PSMA-HBED-CC uptake in the cerebellum on PET/CT, which was confirmed histopathologically as a hemangioblastoma [81].

**3.4.5. PSMA in Other CNS Tumors Summary.** In summary, PSMA-targeting PET showed uptake in prostate cancer CNS metastases with variable avidity. Only case reports and small case series have been published though, and there is a need for systematic study of this imaging modality in this patient population. Anecdotal PSMA-targeted PET imaging has also shown uptake in brain metastases from breast cancer, RCC brain, melanoma, and lung cancer. There are also a few reports of  $^{68}\text{Ga}$ -tagged PSMA-targeted tracer uptake in meningiomas, though more research is needed to understand the potential use of this imaging modality in meningiomas.

### 3.5. Potential Therapeutic and Theragnostic Applications of PSMA

**3.5.1. Labeled Alpha-Ray Emitting Radioisotopes.**  $^{225}\text{Ac}$ -PSMA-617 is an alpha-emitting radioisotope-labeled derivative of PSMA-617, which targets the overexpressed PSMA seen in prostate cancer, and this therapy has demonstrated excellent therapeutic response in prostate cancer [82, 83]. It was also recently noted to be effective in the treatment of prostate cancer brain metastases [64]. Initial assessment with  $^{68}\text{Ga}$ -PSMA PET revealed cerebral metastases, and then, following one and two cycles of 8 MBq of  $^{225}\text{Ac}$ -PSMA-617 treatment, there was a functional response on  $^{68}\text{Ga}$ -PSMA PET. The serum PSA level dropped from an ini-

tial 788.63  $\mu\text{g/L}$  to 6.52  $\mu\text{g/L}$ , to 0.32  $\mu\text{g/L}$ . This incidental finding demonstrates the potential for this prostate cancer therapy to be applied in brain metastases and perhaps other PSMA-expressing CNS tumors as well (Figure 6).

**3.5.2. Labeled Beta-Ray Emitting Radioisotopes.**  $^{177}\text{Lu}$  is a beta-emitting radioisotope, and  $^{177}\text{Lu}$ -PSMA-617 targets overexpressed PSMA and has demonstrated excellent therapeutic response in metastatic prostate cancer [84]. The first report of  $^{177}\text{Lu}$ -PSMA-617 therapy use in prostate cancer brain metastases came from Wei et al., in which they report significant regression of cerebral lesions following  $^{177}\text{Lu}$ -PSMA-617 treatment plus local radiotherapy in two patients [63]. The first had several radiation-refractory cerebral and cerebellar metastases, which showed  $^{68}\text{Ga}$ -PSMA-11 (HBED-CC) uptake on initial PET imaging. After four cycles of  $^{177}\text{Lu}$ -PSMA-617 therapy totaling 25.5 GBq, the lesions demonstrated reduced size and PSMA expression. This correlated to a decrease in serum PSA from 195 ng/mL to 2.4 ng/mL. The second patient had one brain metastasis that was diagnosed after several hormonal and chemotherapy systemic treatments. This lesion showed  $^{68}\text{Ga}$ -PSMA-11 (HBED-CC) uptake on initial PET, and after three cycles of  $^{177}\text{Lu}$ -PSMA-617 therapy, the first of which was combined with radiotherapy; it had nearly completely regressed. This was accompanied by a decrease in serum PSA from 112 ng/mL to 3.9 ng/mL. Recently, Kumar et al. reported on the successful application of  $^{177}\text{Lu}$ -PSMA-617 therapy in a glioblastoma patient [51]. The patient presented with recurrent disease, which demonstrated intense  $^{68}\text{Ga}$ -PSMA-11 (HBED-CC) uptake in the MRI-enhancing areas. The patient underwent three cycles of  $^{177}\text{Lu}$ -PSMA-617 for a total dose of 3700 MBq, after which MRI and  $^{68}\text{Ga}$ -PSMA-11 (HBED-CC) PET demonstrated a reduction in lesion size (from 18 mL to 5.4 mL), which was accompanied by an improvement in ECOG score from 4 to 3. These positive results are tempered by a recent report from Parihar et al., which showed the emergence of new brain

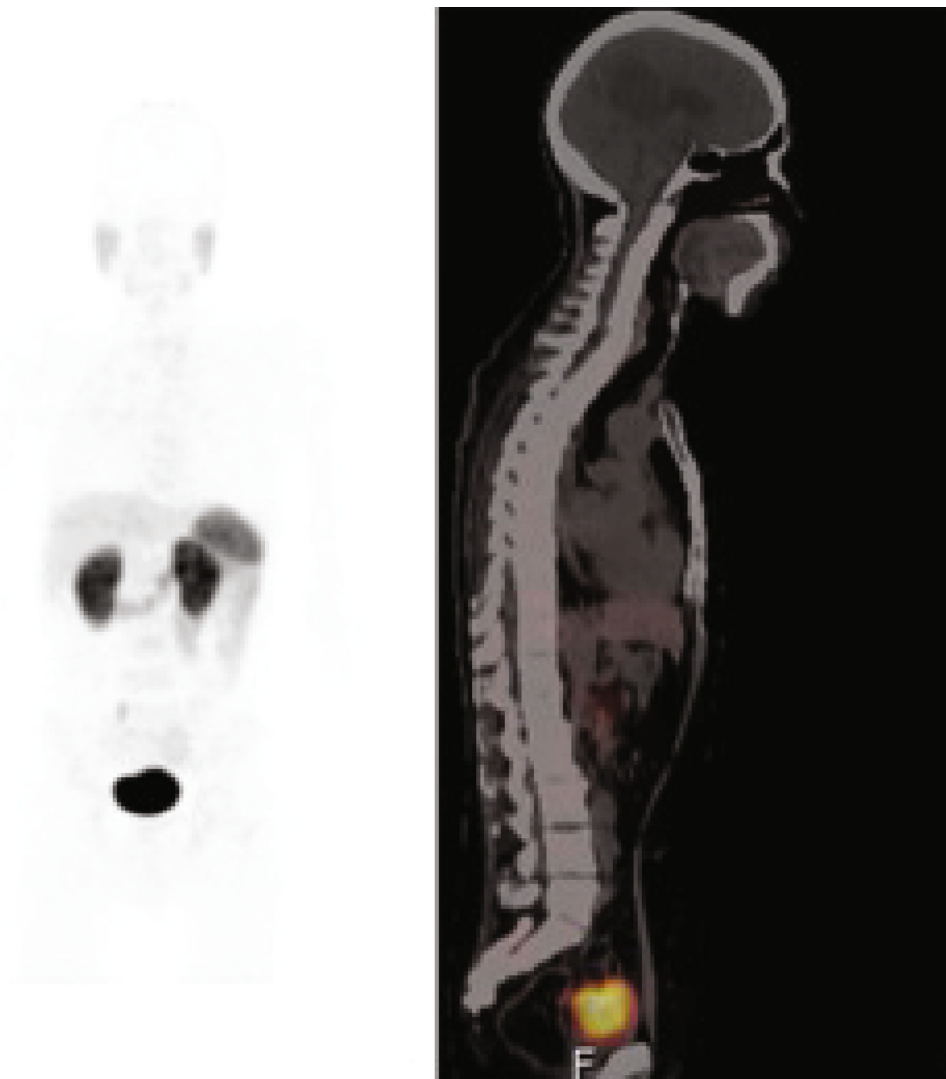




(a)

FIGURE 6: Continued.





(b)

FIGURE 6: Response to  $^{225}\text{Ac}$ -PSMA-617 therapy in a representative prostate cancer brain metastasis. (a) Pretreatment  $^{68}\text{Ga}$ -PSMA PET/CT. (b) Restaging PSMA PET/CT scan after one cycle of  $^{225}\text{Ac}$ -PSMA. Reproduced with permission from Sathekge et al. [64].

metastasis with  $^{68}\text{Ga}$ -PSMA uptake, after  $^{177}\text{Lu}$ -PSMA and  $^{225}\text{Ac}$ -PSMA treatment of prostate cancer [65].

**3.5.3. MRI-Guided Focused Ultrasound.** MRI-guided focused ultrasound (MRgFUS) has been leveraged as a tool for disrupting the blood-brain barrier (BBB) in order to permit the passage of drugs, for a number of CNS indications [85]. In a preclinical study of nine rats with nondiseased brains, Airan et al. demonstrated that  $^{18}\text{F}$ -DCFPyL could be administered and targeted to a specific brain focus using MRgFUS for BBB disruption [86]. Following MRgFUS,  $^{18}\text{F}$ -DCFPyL uptake localized to the foci of BBB disruption and extended minimally beyond the contrast-enhancing MRI lesion. Target uptake plateaued at 80 minutes postadministration, with a maximal TBR of 7. PSMA-binding specificity was confirmed by administering the anti-PSMA ZJ-43 which lowered TBR fourfold. Although this was performed on healthy brains, it demonstrated the possibility of leveraging MRgFUS

for opening the BBB to allow hydrophilic  $^{18}\text{F}$ -DCFPyL PSMA to enter and reach target tissue within the brain.

#### 4. Future Objectives

The PSMA-binding tracer mechanism of expression is thought to be specific to tumor vasculature, not to invading or proliferating cells. While this may limit its utility as an isolated imaging modality, it may prove to be a useful adjunct to other neuroimaging modalities for CNS tumors. On the other hand, the significant potential advantage of PSMA-targeted PET tracers is in CNS tumor theranostics, which the current literature only begins to describe. There may be the potential for a wide range of future applications, such as small molecule selective PSMA inhibitors and radiosensitizers. Pairing PSMA-targeted diagnostic imaging with PSMA-targeted therapeutics may yield a robust theragnostic option for CNS tumor patients.

## 5. Conclusions

In summary, this systematic review of the literature on PSMA-targeted tracer use in CNS tumors demonstrates promising results about the potential for this PET tracer for neuro-oncologic imaging. Future efforts should continue to explore the potential for PSMA in neuro-oncologic imaging, specifically focusing on proposed mechanism(s) of PSMA expression in CNS tumors, differential imaging performance by CNS tumor type, direct comparison of PSMA-targeted PET to other neuroimaging modalities for diagnosing and monitoring CNS tumors, and direct comparison of competing PSMA-binding radiotracers. The surreptitious discovery of the utility of PSMA-targeted PET imaging in CNS tumors has invigorated much excitement in the field about its potential clinical application, but more research is needed to better understand this PET tracer before it can be implemented clinically.

## Abbreviations

AUC:	Area under the ROC curve
BBB:	Blood-brain barrier
CNS:	Central nervous system
CT:	Computerized tomography
<sup>18</sup> F-DCFpyL:	2-(3-(1-Carboxy-5-(6-[ <sup>18</sup> F]fluoro-pyridine-3-carbonyl)-amino-pentyl)-ureido)-pentanedioic acid
FDG:	Fluorodeoxyglucose
GBM:	Glioblastoma
GCPII:	Glutamate carboxypeptidase II
HGG:	High-grade glioma
IHC:	Immunohistochemistry
LGG:	Low-grade glioma
mAb:	Monoclonal antibody
MRgFUS:	MRI-guided focused ultrasound
MRI:	Magnetic resonance imaging
NAAG:	N-Acetyl-L-aspartyl-L-glutamate
PCNSL:	Primary central nervous system lymphoma
PET:	Positron emission tomography
PMPA:	PSMA-receptor inhibitor 2-(phosphonomethyl)pentane-1,5-dioic acid
PSMA:	Prostate-specific membrane antigen
SPECT:	Single-photon emission computerized tomography
SUV:	Standardized uptake value
TBR:	Tumor to background ratio
VWF:	von Willebrand factor
<sup>89</sup> Zr-Df-IAB2M:	<sup>89</sup> Zirconium-desferrioxamine anti-PSMA minibody.

## Data Availability

The data supporting this systematic review article are from previously reported studies included within the article and which have been cited.

## Conflicts of Interest

The authors declare no potential conflicts of interest with respect to the research, authorship, and/or publication of this article.

## Authors' Contributions

All authors have made substantial contributions to this study and manuscript, as follows: conceived the study idea and provided guidance and oversight to the project: JC, CJ, CR, MW, and JK; made substantial contributions to the study planning: BS, JC, CJ, and JK; conducted the literature review, data collection and analysis, and manuscript drafting: BS, JC, CJ, and JK; critically reviewed and revised the manuscript for important intellectual content: BS, JC, CJ, CR, MW, and JK; approved the submission of this final version of the manuscript and agreed to be accountable for all aspects of the work regarding its accuracy and integrity: BS, JC, CJ, CR, and MW, and JK.

## References

- [1] H. Nandu, P. Y. Wen, and R. Y. Huang, "Imaging in neuro-oncology," *Therapeutic Advances in Neurological Disorders*, vol. 11, 2018.
- [2] M. Inubushi, H. Miura, I. Kuji, K. Ito, and R. Minamimoto, "Current status of radioligand therapy and positron-emission tomography with prostate-specific membrane antigen," *Annals of Nuclear Medicine*, vol. 34, pp. 879–883, 2020.
- [3] P. Backhaus, B. Noto, N. Avramovic et al., "Targeting PSMA by radioligands in non-prostate disease-current status and future perspectives," *European Journal of Nuclear Medicine and Molecular Imaging*, vol. 45, no. 5, pp. 860–877, 2018.
- [4] R. A. Salas Fragomeni, T. Amir, S. Sheikhabaehi et al., "Imaging of nonprostate cancers using PSMA-targeted radiotracers: rationale, current state of the field, and a call to arms," *Journal of Nuclear Medicine*, vol. 59, pp. 871–877, 2018.
- [5] C. Van de Wiele, M. Sathekge, B. de Spiegeleer, P. de Jonghe, L. Beels, and A. Maes, "PSMA-targeting positron emission agents for imaging solid tumors other than non-prostate carcinoma: a systematic review," *International Journal of Molecular Sciences*, vol. 20, no. 19, p. 4886, 2019.
- [6] P. Šácha, J. Zámečník, C. Bařinka et al., "Expression of glutamate carboxypeptidase II in human brain," *Neuroscience*, vol. 144, no. 4, pp. 1361–1372, 2007.
- [7] M. B. Robinson, R. D. Blakely, and J. T. Coyle, "Quisqualate selectively inhibits a brain peptidase which cleaves N-acetyl-L-aspartyl-L-glutamate in vitro," *European Journal of Pharmacology*, vol. 130, no. 3, pp. 345–347, 1986.
- [8] U. V. Berger, R. Luthi-Carter, L. A. Passani et al., "Glutamate carboxypeptidase II is expressed by astrocytes in the adult rat nervous system," *The Journal of Comparative Neurology*, vol. 415, no. 1, pp. 52–64, 1999.
- [9] K. A. Rahn, C. C. Watkins, J. Alt et al., "Inhibition of glutamate carboxypeptidase II (GCPII) activity as a treatment for cognitive impairment in multiple sclerosis," *Proceedings of the National Academy of Sciences of the United States of America*, vol. 109, pp. 20101–20106, 2012.
- [10] J. J. Vornov, D. Peters, M. Nedelcovych, K. Hollinger, R. Rais, and B. S. Slusher, "Looking for drugs in all the wrong places:

- use of GCPII inhibitors outside the brain,” *Neurochemical Research*, vol. 45, no. 6, pp. 1256–1267, 2020.
- [11] V. Cuccurullo, G. D. di Stasio, L. Evangelista, A. Ciarmiello, and L. Mansi, “Will  $^{68}\text{Ga}$  PSMA-radioligands be the only choice for nuclear medicine in prostate cancer in the near future? A clinical update,” *Revista Española de Medicina Nuclear e Imagen Molecular*, vol. 37, no. 2, pp. 103–109, 2018.
  - [12] I. Dijkgraaf and O. C. Boerman, “Radionuclide imaging of tumor angiogenesis,” *Cancer Biotherapy & Radiopharmaceuticals*, vol. 24, no. 6, pp. 637–647, 2009.
  - [13] S. S. Chang, V. E. Reuter, W. D. W. Heston, N. H. Bander, L. S. Grauer, and P. B. Gaudin, “Five different anti-prostate-specific membrane antigen (PSMA) antibodies confirm PSMA expression in tumor-associated neovasculature,” *Cancer Research*, vol. 59, no. 13, pp. 3192–3198, 1999.
  - [14] A. G. Wernicke, M. A. Edgar, E. Lavi et al., “Prostate-specific membrane antigen as a potential novel vascular target for treatment of glioblastoma multiforme,” *Archives of Pathology & Laboratory Medicine*, vol. 135, no. 11, pp. 1486–1489, 2011.
  - [15] A. G. Wernicke, S. Varma, E. A. Greenwood et al., “Prostate-specific membrane antigen expression in tumor-associated vasculature of breast cancers,” *APMIS*, vol. 122, no. 6, pp. 482–489, 2014.
  - [16] N. Nomura, S. Pastorino, P. Jiang et al., “Prostate specific membrane antigen (PSMA) expression in primary gliomas and breast cancer brain metastases,” *Cancer Cell International*, vol. 14, no. 1, 2014.
  - [17] J. Schwenck, G. Tabatabai, M. Skardelly et al., “In vivo visualization of prostate-specific membrane antigen in glioblastoma,” *European Journal of Nuclear Medicine and Molecular Imaging*, vol. 42, no. 1, pp. 170–171, 2015.
  - [18] M. Unterrainer, M. Niyazi, V. Ruf, P. Bartenstein, and N. L. Albert, “The endothelial prostate-specific membrane antigen is highly expressed in gliosarcoma and visualized by [ $^{68}\text{Ga}$ ]-PSMA-11 PET: a theranostic outlook for brain tumor patients?,” *Neuro-Oncology*, vol. 19, no. 12, pp. 1698–1699, 2017.
  - [19] R. A. Salas Fragomeni, J. R. Menke, M. Holdhoff et al., “Prostate-specific membrane antigen-targeted imaging with [ $^{18}\text{F}$ ]DCFPyL in high-grade gliomas,” *Clinical Nuclear Medicine*, vol. 42, no. 10, pp. e433–e435, 2017.
  - [20] M. Matsuda, E. Ishikawa, T. Yamamoto et al., “Potential use of prostate specific membrane antigen (PSMA) for detecting the tumor neovasculature of brain tumors by PET imaging with  $^{89}\text{Zr}$ -Df-IAB2M anti-PSMA minibody,” *Journal of Neuro-Oncology*, vol. 138, no. 3, pp. 581–589, 2018.
  - [21] H. Saffar, M. Noohi, S. M. Tavangar, H. Saffar, and S. Azimi, “Expression of prostate-specific membrane antigen (PSMA) in brain glioma and its correlation with tumor grade,” *Iranian Journal of Pathology*, vol. 13, no. 1, pp. 45–53, 2018.
  - [22] P. Mahzouni and M. Shavakhi, “Prostate-specific membrane antigen expression in neovasculature of glioblastoma multiforme,” *Advanced Biomedical Research*, vol. 8, 2019.
  - [23] D. Oliveira, C. Stegmayr, A. Heinzel et al., “High uptake of  $^{68}\text{Ga}$ -PSMA and  $^{18}\text{F}$ -DCFPyL in the peritumoral area of rat gliomas due to activated astrocytes,” *EJNMMI Research*, vol. 10, no. 1, p. 55, 2020.
  - [24] D. Liu, G. Cheng, X. Ma et al., “PET/CT using  $^{68}\text{Ga}$ -PSMA-617 versus  $^{18}\text{F}$ -fluorodeoxyglucose to differentiate low- and high-grade gliomas,” *Journal of Neuroimaging*, vol. 31, no. 4, pp. 733–742, 2021.
  - [25] A. Holzgreve, A. Biczok, V. C. Ruf et al., “PSMA expression in glioblastoma as a basis for theranostic approaches: a retrospective, correlational panel study including immunohistochemistry, clinical parameters and PET imaging,” *Frontiers in Oncology*, vol. 11, article 646387, 2021.
  - [26] M. P. S. Dunphy and N. Pillarsetty, “The unique pharmacometrics of small molecule therapeutic drug tracer imaging for clinical oncology,” *Cancers*, vol. 12, no. 9, p. 2712, 2020.
  - [27] U. Tateishi, “Prostate-specific membrane antigen (PSMA)-ligand positron emission tomography and radioligand therapy (RLT) of prostate cancer,” *Japanese Journal of Clinical Oncology*, vol. 50, no. 4, pp. 349–356, 2020.
  - [28] J. D. Young, V. Abbate, C. Imberti et al., “ $^{68}\text{Ga}$ -THP-PSMA: a PET imaging agent for prostate cancer offering rapid, room-temperature, 1-step kit-based radiolabeling,” *Journal of Nuclear Medicine*, vol. 58, no. 8, pp. 1270–1277, 2017.
  - [29] M. Czarniecki, E. Mena, L. Lindenberg et al., “Keeping up with the prostate-specific membrane antigens (PSMAs): an introduction to a new class of positron emission tomography (PET) imaging agents,” *Translational Andrology and Urology*, vol. 7, no. 5, pp. 831–843, 2018.
  - [30] L. Martinova, L. De Palatis, E. Etchebehere, and G. Ravizzini, “Gallium-68 in medical imaging,” *Current Radiopharmaceuticals*, vol. 9, no. 3, pp. 187–207, 2016.
  - [31] F. L. Giesel, L. Will, I. Lawal et al., “Intraindividual comparison of  $^{18}\text{F}$ -PSMA-1007 and  $^{18}\text{F}$ -DCFPyL PET/CT in the prospective evaluation of patients with newly diagnosed prostate carcinoma: a pilot study,” *Journal of Nuclear Medicine*, vol. 59, no. 7, pp. 1076–1080, 2018.
  - [32] S. Rowe, D. Holt, E. Antonarakis et al., “[ $^{18}\text{F}$ ]DCFBC (DCFBC) prostate specific membrane antigen (PSMA) based PET/CT detection of metastatic castration-sensitive (CSPC) and castration-resistant prostate cancer (CRPC),” *Journal of Nuclear Medicine*, vol. 55, p. 19, 2014.
  - [33] C. Cui, F. Wang, M.-R. Zhang et al., “Synthesis, biodistribution and metabolic analysis of  $^{64}\text{Cu}$  labeled PSMA-targeted ligand,” *Journal of Nuclear Medicine*, vol. 57, p. 1385, 2016.
  - [34] C. M. Zechmann, A. Afshar-Oromieh, T. Armor et al., “Radiation dosimetry and first therapy results with a  $^{124}\text{I}/^{131}\text{I}$ -labeled small molecule (MIP-1095) targeting PSMA for prostate cancer therapy,” *European Journal of Nuclear Medicine and Molecular Imaging*, vol. 41, no. 7, pp. 1280–1292, 2014.
  - [35] N. Pandit-Taskar, J. A. O’Donoghue, S. Ruan et al., “First-in-human imaging with  $^{89}\text{Zr}$ -Df-IAB2M anti-PSMA minibody in patients with metastatic prostate cancer: pharmacokinetics, biodistribution, dosimetry, and lesion uptake,” *Journal of Nuclear Medicine*, vol. 57, no. 12, pp. 1858–1864, 2016.
  - [36] Y. Zhang, H. Hong, and W. Cai, “PET tracers based on zirconium-89,” *Current Radiopharmaceuticals*, vol. 4, no. 2, pp. 131–139, 2011.
  - [37] B. Albaloooshi, M. Al Sharhan, F. Bagheri et al., “Direct comparison of  $^{99\text{m}}\text{Tc}$ -PSMA SPECT/CT and  $^{68}\text{Ga}$ -PSMA PET/CT in patients with prostate cancer,” *Asia Oceania Journal of Nuclear Medicine and Biology*, vol. 8, no. 1, pp. 1–7, 2020.
  - [38] C. Schmidkonz, C. Hollweg, M. Beck et al., “ $^{99\text{m}}\text{Tc}$ -MIP-1404-SPECT/CT for the detection of PSMA-positive lesions in 225 patients with biochemical recurrence of prostate cancer,” *The Prostate*, vol. 78, no. 1, pp. 54–63, 2018.
  - [39] S. Vallabhajosula, A. Nikolopoulou, J. W. Babich et al., “ $^{99\text{m}}\text{Tc}$ -labeled small-molecule inhibitors of prostate-specific membrane antigen: pharmacokinetics and biodistribution

- studies in healthy subjects and patients with metastatic prostate cancer,” *Journal of Nuclear Medicine*, vol. 55, no. 11, pp. 1791–1798, 2014.
- [40] P. Werner, C. Neumann, M. Eiber, H. J. Wester, and M. Schottelius, “[<sup>99m</sup>Tc]Tc-PSMA-I&S-SPECT/CT: experience in prostate cancer imaging in an outpatient center,” *EJNMMI Research*, vol. 10, no. 1, p. 45, 2020.
- [41] F. O. Garcia-Perez, J. Davanzo, S. Lopez-Buenrostro et al., “Head to head comparison performance of <sup>99m</sup>Tc-EDDA/HYNIC-iPSMA SPECT/CT and <sup>68</sup>Ga-PSMA-11 PET/CT a prospective study in biochemical recurrence prostate cancer patients,” *American Journal of Nuclear Medicine and Molecular Imaging*, vol. 8, no. 5, pp. 332–340, 2018.
- [42] A. Sasikumar, A. Joy, M. R. Pillai et al., “Diagnostic value of <sup>68</sup>Ga PSMA-11 PET/CT imaging of brain tumors-preliminary analysis,” *Clinical Nuclear Medicine*, vol. 42, no. 1, pp. e41–e48, 2017.
- [43] A. Sasikumar, R. Kashyap, A. Joy et al., “Utility of <sup>68</sup>Ga-PSMA-11 PET/CT in imaging of glioma-a pilot study,” *Clinical Nuclear Medicine*, vol. 43, no. 9, pp. e304–e309, 2018.
- [44] J. Kunikowska, K. Bartosz, and K. Leszek, “Glioblastoma multiforme: another potential application for <sup>68</sup>Ga-PSMA PET/CT as a guide for targeted therapy,” *European Journal of Nuclear Medicine and Molecular Imaging*, vol. 45, pp. 886–887, 2018.
- [45] D. Malik, R. Kumar, B. R. Mittal, H. Singh, A. Bhattacharya, and S. K. Singh, “<sup>68</sup>Ga-labeled PSMA uptake in nonprostatic malignancies: has the time come to remove “PS” From PSMA?,” *Clinical Nuclear Medicine*, vol. 43, no. 7, pp. 529–532, 2018.
- [46] P. Verma, G. Malhotra, A. Goel et al., “Differential uptake of <sup>68</sup>Ga-PSMA-HBED-CC (PSMA-11) in low-grade versus high-grade gliomas in treatment-naive patients,” *Clinical Nuclear Medicine*, vol. 44, no. 5, pp. e318–e322, 2019.
- [47] M. Gupta, P. S. Choudhury, I. C. Premsagar, M. Gairola, and P. Ahlawat, “Role of <sup>68</sup>Ga-prostate-specific membrane antigen PET/CT in disease assessment in glioblastoma within 48 hours of surgery,” *Clinical Nuclear Medicine*, vol. 45, no. 3, pp. 204–205, 2020.
- [48] A. Moreau, E. Marie, A. Bonneville-Levard, A. Basle, and D. Kryza, “Skull vault hemangioma mimicking neoplastic lesion on [(68)Ga]Ga-PSMA-11 PET/CT in a patient with glioblastoma: a case report,” *Radiology Case Reports*, 2020.
- [49] B. Pernthaler, T. Nazerani Hooshmand, J. Igrec, H. Kvaternik, and R. M. Aigner, “Oligodendroglioma in <sup>68</sup>Ga-PSMA-11 and <sup>18</sup>F-Fluciclovine PET/CT,” *Clinical Nuclear Medicine*, vol. 46, no. 4, pp. e231–e232, 2021.
- [50] E. Pilati, D. G. Nicolotti, F. Ceci et al., “<sup>68</sup>Ga-prostate-specific membrane antigen 11 PET/CT detects residual glioblastoma after radical surgery in a patient with synchronous recurrent prostate cancer: a case report,” *Clinical Nuclear Medicine*, vol. 45, pp. e151–e153, 2020.
- [51] A. Kumar, S. Ballal, M. P. Yadav et al., “<sup>177</sup>Lu-/<sup>68</sup>Ga-PSMA theranostics in recurrent glioblastoma multiforme: proof of concept,” *Clinical Nuclear Medicine*, vol. 45, no. 12, pp. e512–e513.
- [52] X. Zhang, J. Yuan, C. Zhou, and W. Fan, “Diagnose of glioma using <sup>68</sup>Ga-PSMA and <sup>18</sup>F-FDG PET/MRI,” *Japanese Journal of Clinical Oncology*, vol. 51, no. 3, pp. 506–508, 2021.
- [53] J. Kunikowska, R. Kulinski, K. Muylle, H. Koziara, and L. Króllicki, “<sup>68</sup>Ga-prostate-specific membrane antigen-11 PET/CT: a new imaging option for recurrent glioblastoma multiforme?,” *Clinical Nuclear Medicine*, vol. 45, no. 1, pp. 11–18, 2020.
- [54] B. M. Stopa, C. Juhász, and S. Mittal, “Comparison of amino acid PET to advanced and emerging MRI techniques for neurooncology imaging: a systematic review of the recent studies,” *Molecular Imaging*, vol. 2021, pp. 1–19, 2021.
- [55] E. Akgun, M. Y. Akgun, H. H. Selçuk, M. Uzan, and H. B. Sayman, “<sup>68</sup>Ga PSMA PET/MR in the differentiation of low and high grade gliomas: Is <sup>68</sup>Ga PSMA PET/MRI useful to detect brain gliomas?,” *European Journal of Radiology*, vol. 130, article 109199, 2020.
- [56] F. Marafi, A. Sasikumar, W. Fathallah, and A. Esmail, “<sup>18</sup>F-PSMA 1007 brain PET/CT imaging in glioma recurrence,” *Clinical Nuclear Medicine*, vol. 45, no. 1, pp. e61–e62, 2020.
- [57] P. S. Chakraborty, R. Kumar, M. Tripathi, C. J. Das, and C. Bal, “Detection of brain metastasis with <sup>68</sup>Ga-labeled PSMA ligand PET:CT a novel radiotracer for imaging of prostate carcinoma,” *Clinical Nuclear Medicine*, vol. 40, no. 4, pp. 328–329, 2015.
- [58] S. Dureja, P. Thakral, V. Pant, and I. Sen, “Rare sites of metastases in prostate cancer detected on Ga-68 PSMA PET/CT scan-a case series,” *Indian Journal of Nuclear Medicine*, vol. 32, no. 1, p. 13, 2017.
- [59] W. Langsteger, F. Fitz, A. Rezaee, H. Geinitz, and M. Beheshti, “<sup>68</sup>Ga-PSMA PET/CT with MRI fusion: spinal cord metastasis from prostate cancer,” *European Journal of Nuclear Medicine and Molecular Imaging*, vol. 44, no. 2, pp. 348–349, 2017.
- [60] M. Chan, E. Hsiao, and J. Turner, “Cerebellar metastases from prostate cancer on <sup>68</sup>Ga-PSMA PET/CT,” *Clinical Nuclear Medicine*, vol. 42, no. 3, pp. 193–194, 2017.
- [61] M. I. Ross, N. Bird, I. A. Mendichovszky, and Y. L. Rimmer, “Neurologically asymptomatic cerebral oligometastatic prostate carcinoma metastasis identified on [Ga]Ga-THP-PSMA PET/CT,” *EJNMMI Research*, vol. 10, no. 1, p. 108, 2020.
- [62] C. Yin, B. Ho, L. Chan, and L. Emmett, “Asymptomatic prostate cancer brain metastases on <sup>68</sup>Ga-PSMA PET/CT,” *Clinical Nuclear Medicine*, vol. 44, no. 6, pp. e382–e384, 2019.
- [63] X. Wei, C. Schlenkhoff, B. Schwarz, M. Essler, and H. Ahmadzadehfhar, “Combination of <sup>177</sup>Lu-PSMA-617 and external radiotherapy for the treatment of cerebral metastases in patients with castration-resistant metastatic prostate cancer,” *Clinical Nuclear Medicine*, vol. 42, no. 9, pp. 704–706, 2017.
- [64] M. M. Satheke, F. Bruchertseifer, I. O. Lawal et al., “Treatment of brain metastases of castration-resistant prostate cancer with <sup>225</sup>Ac-PSMA-617,” *European Journal of Nuclear Medicine and Molecular Imaging*, vol. 46, no. 8, pp. 1756–1757, 2019.
- [65] A. S. Parihar, K. R. Chandekar, H. Singh, A. Sood, and B. R. Mittal, “Orbital and brain metastases on (68)Ga-PSMA PET/CT in a patient with prostate carcinoma refractory to (177)Lu-PSMA and (225)Ac-PSMA therapy,” *Asia Oceania Journal of Nuclear Medicine and Biology*, 2021.
- [66] R. McBean, A. Tatkovc, and D. C. Wong, “Intracranial metastasis from prostate cancer: investigation, incidence, and imaging findings in a large cohort of Australian men,” *Journal of Clinical Imaging Science*, vol. 11, p. 24, 2021.
- [67] S. S. Medina-Ornelas, F. O. García-Pérez, C. Medel-Gamez, and E. Paredes-Amoroto, “A single brain metastasis seen on <sup>68</sup>Ga-PSMA PET/CT in recurrent of breast cancer,” *Revista*



- Española de Medicina Nuclear e Imagen Molecular*, vol. 37, pp. 61–62, 2018.
- [68] F. Marafi, A. Sasikumar, M. Alfeeli, and W. Fathallah, “18F-PSMA 1007 uptake in brain metastases from breast cancer,” *Clinical Nuclear Medicine*, vol. 45, no. 2, pp. e77–e79, 2020.
- [69] E. Arslan, N. Ergül, Y. Karagöz, A. A. Gedik, and T. F. Çermik, “Recurrent brain metastasis of triple negative breast cancer with high uptake in 68Ga-PSMA-11 PET/CT,” *Clinical Nuclear Medicine*, vol. 46, pp. e106–e108, 2021.
- [70] S. P. Rowe, M. A. Gorin, H. J. Hammers et al., “Imaging of metastatic clear cell renal cell carcinoma with PSMA-targeted 18F-DCFPyL PET/CT,” *Annals of Nuclear Medicine*, vol. 29, no. 10, pp. 877–882, 2015.
- [71] Y. Yin, S. P. Campbell, M. C. Markowski et al., “Inconsistent detection of sites of metastatic non-clear cell renal cell carcinoma with PSMA-targeted [18F]DCFPyL PET/CT,” *Molecular Imaging and Biology*, vol. 21, no. 3, pp. 567–573, 2019.
- [72] N. Hod, S. Lantsberg, E. Benkovich, D. E. Kazap, M. Preiskel, and D. Levin, “Incidental detection of malignant melanoma brain recurrence on 68Ga-prostate-specific membrane antigen PET/CT,” *Clinical Nuclear Medicine*, vol. 45, no. 11, pp. 896–899, 2020.
- [73] R. Bilgin, N. Ergül, and T. F. Çermik, “Incidental meningioma mimicking metastasis of prostate adenocarcinoma in 68Ga-labeled PSMA ligand PET/CT,” *Clinical Nuclear Medicine*, vol. 41, no. 12, pp. 956–958, 2016.
- [74] T. K. Jain, A. G. S. Jois, V. S. Kumar, and B. R. Mittal, “Deteccion incidental de afeidez de trazador en meningioma en <sup>68</sup>Ga-PSMA PET/TC durante la estratificacion inicial de un cancer de prostata,” *Revista Española de Medicina Nuclear e Imagen Molecular (English Edition)*, vol. 36, no. 2, pp. 133–134, 2017.
- [75] N. Gupta, R. Verma, and E. S. Belho, “Prostate-specific membrane antigen-avid meningioma detected in 68Ga-prostate-specific membrane antigen PET/CT,” *Clinical Nuclear Medicine*, vol. 45, pp. 692–693, 2020.
- [76] M. Courtney, C. Johnston, and A. Nasoodi, “Meningioma uptake of (68)Gallium-PSMA-11 as a pitfall on positron emission tomography/computer tomography,” *Acta Radiologica Open*, vol. 10, 2021.
- [77] M. Z. Junqueira, N. H. Rocha, and M. T. Sapienza, “68Ga-prostate-specific membrane antigen PET/CT uptake in intraventricular meningioma in the choroid plexus,” *Clinical Nuclear Medicine*, vol. 46, no. 1, pp. 58–59, 2021.
- [78] F. Calabria, V. Gangemi, D. Gullà, O. Schillaci, and G. L. Cascini, “Captacion de <sup>64</sup>Cu-PSMA en un meningioma: falso positivo de un radiofarmaco prometedor,” *Revista Espanola De Medicina Nuclear E Imagen Molecular*, vol. 36, no. 5, pp. 335–336, 2017.
- [79] M. Haemels, S. Jentjens, F. Cleeren et al., “All that glitters is not prostate cancer- incidental finding of PSMA-avid meningioma,” *Hellenic Journal Of Nuclear Medicine*, vol. 23, no. 1, pp. 79–80, 2020.
- [80] K. C. Patro, M. Palla, and R. Kashyap, “Unusual case of metastatic intracranial hemangiopericytoma and emphasis on role of 68Ga-PSMA PET in imaging,” *Clinical Nuclear Medicine*, vol. 43, no. 9, pp. e331–e333, 2018.
- [81] N. Gohimont, P. J. Tchofo, M.-L. Racu et al., “Hemangioblastoma,” *Clinical Nuclear Medicine*, vol. 46, no. 6, pp. 485–487, 2021.
- [82] M. P. Yadav, S. Ballal, R. K. Sahoo, M. Tripathi, A. Seth, and C. Bal, “Efficacy and safety of (225)Ac-PSMA-617 targeted alpha therapy in metastatic castration-resistant prostate cancer patients,” *Theranostics*, vol. 10, pp. 9364–9377, 2020.
- [83] S. Agrawal, “The role of 225Ac-PSMA-617 in chemotherapy-naive patients with advanced prostate cancer: is it the new beginning,” *Indian Journal of Urology*, vol. 36, pp. 69–70, 2020.
- [84] M. Sun, M. O. Niaz, A. Nelson, M. Skafida, and M. J. Niaz, “Review of 177Lu-PSMA-617 in patients with metastatic castration-resistant prostate cancer,” *Cureus*, vol. 12, article e8921, 2020.
- [85] L. Lamsam, E. Johnson, I. D. Connolly, M. Wintermark, and M. H. Gephart, “A review of potential applications of MR-guided focused ultrasound for targeting brain tumor therapy,” *Neurosurgical Focus*, vol. 44, p. E10, 2018.
- [86] R. D. Airan, C. A. Foss, N. P. Ellens et al., “MR-guided delivery of hydrophilic molecular imaging agents across the blood-brain barrier through focused ultrasound,” *Molecular Imaging and Biology*, vol. 19, pp. 24–30, 2017.
- [87] S. M. Hillier, K. P. Maresca, G. Lu et al., “<sup>99m</sup>Tc-labeled small-molecule inhibitors of prostate-specific membrane antigen for molecular imaging of prostate cancer,” *Journal of Nuclear Medicine*, vol. 54, no. 8, pp. 1369–1376, 2013.
- [88] J. Zhang, J. Zhang, X. Xu et al., “Evaluation of radiation dosimetry of <sup>99m</sup>Tc-HYNIC-PSMA and imaging in prostate cancer,” *Scientific Reports*, vol. 10, no. 1, p. 4179, 2020.